

CELLULAR AUTOMATON MODEL OF REACTION-TRANSPORT PROCESSES

T. Karapiperis,
Paul Scherrer Institute, CH-5232 Villigen PSI, Switzerland

B. Blankleider,
Paul Scherrer Institute, CH-5232 Villigen PSI, Switzerland,
*and School of Physical Sciences, Flinders University, Bedford Park, S.A. 5042, Australia**

Abstract

The transport and chemical reactions of solutes are modelled as a cellular automaton in which molecules of different species perform a random walk on a regular lattice and react according to a local probabilistic rule. The model describes advection and diffusion in a simple way, and as no restriction is placed on the number of particles at a lattice site, it is also able to describe a wide variety of chemical reactions. Assuming molecular chaos and a smooth density function, we obtain the standard reaction-transport equations in the continuum limit. Simulations on one- and two-dimensional lattices show that the discrete model can be used to approximate the solutions of the continuum equations. We discuss discrepancies which arise from correlations between molecules and how these disappear as the continuum limit is approached. Of particular interest are simulations displaying long-time behaviour which depends on long-wavelength statistical fluctuations not accounted for by the standard equations. The model is applied to the reactions $a + b \rightleftharpoons c$ and $a + b \rightarrow c$ with homogeneous and inhomogeneous initial conditions as well as to systems subject to autocatalytic reactions and displaying spontaneous formation of spatial concentration patterns.

*Present address

1 Introduction

The transport of aqueous solutions of contaminants in geological media is inextricably coupled with a rich variety of physical and chemical processes. The solutes may decay radioactively, react chemically with each other, sorb on solid surfaces or change the porosity of the host rock by precipitation/dissolution. Modelling an aqueous system in its full complexity constitutes, conceptually and mathematically, a formidable task. A model is essentially defined by selecting, on grounds of usefulness and economy, an appropriate set of dependent variables (e.g. aqueous species concentrations) and writing down the laws (e.g. mass conservation, law of mass action) these variables satisfy. A model intended for practical applications has to be translated subsequently into a usable and efficient computer code.

The model presented here takes advantage of the fact that the migration and chemical transformation of aqueous species consists, at the microscopic level, of processes taking place *in parallel* (i.e. simultaneously at many locations) and *locally* (i.e. involving molecules within a small spatial neighbourhood). Each species is represented by a (large) number of ‘particles’ that move and react according to simple rules mimicking the microscopic behaviour of the actual molecules. The model is implemented as simple computer code suitable for *massively parallel computers*. Our approach contrasts with the standard modelling approach which solves systems of non-linear *partial differential equations (PDE’s)* for macroscopic variables. The latter approach neglects microscopic details by effectively averaging solute properties over a small macroscopic volume and dealing only with their local mean values.

Reaction-transport processes are modelled here, following Refs. [1, 2], as a *cellular automaton (CA)*. In general, a *CA* is a *dynamical system which consists of a discrete-valued field defined at the sites of a regular lattice and evolving in discrete time steps, with the field value at a site being determined for the next time step by its present values in a neighbourhood of the site of interest* [3]. In this work, particles reside on the sites of a regular lattice; they move randomly between neighbouring sites, in discrete time steps, and react with a certain probability upon meeting. Formally, this is described

by a set of *occupation numbers*, i.e. an integer-valued field with a species label, giving the number of particles of the different species at each lattice site and evolving in time according to a local rule. The evolution rule consists of a ‘transport’ operation followed by a ‘reaction’ operation. The two operations are repeated iteratively for consecutive time steps. Each operation amounts to applying a simple algorithm on all sites of the lattice simultaneously. The ‘transport’ algorithm prescribes the probability with which a particle will move to a neighbouring site; the probability may depend on species label, location on the lattice, spatial direction or time; in the end, each particle performs a random walk. The ‘reaction’ algorithm, on the other hand, provides the probability with which a given combination of occupation numbers will lead to chemical reaction. We define macroscopic quantities by averaging over an *ensemble* of independent copies of the system of interest. *Particle density*, defined as an ensemble average of the occupation number, obeys a discrete evolution equation. If chemical reactions are present in this equation, occupation numbers can be entirely eliminated in favour of locally averaged particle densities only if certain important conditions are met. As will be discussed in detail in Section 2, one has to assume that the chemical reactions do not give rise to correlations among different species and that the spatial dependence of macroscopic quantities is sufficiently smooth. The *continuum limit* of the resulting equation (i.e. when lattice spacing and time step go to zero) contains the standard advection, diffusion and reaction terms of the macroscopic PDE’s¹. The probabilities of motion and reaction can be chosen so that the desired macroscopic physical and chemical parameters are obtained.

The standard way to model reaction-transport phenomena consists in applying (i) *local mass conservation* to derive a set of partial differential equations, and (ii) *local chemical equilibrium*, according to the law of mass action, to derive a set of non-linear algebraic equations (assuming implicitly that chemical equilibrium is attained instantaneously across the averaging volume on the time scale of the transport processes). The ensuing system

¹For brevity we shall talk about ‘diffusion’, although, in the cases of interest to us, it is *mechanical dispersion*, rather than *molecular diffusion*, that accounts overwhelmingly for the *coefficient of hydrodynamic dispersion*. To the extent that mechanical dispersion can be described by an effective diffusion term, the two processes are indistinguishable from the modelling point of view; naturally, the interpretation of the effective coefficient is very different in the two cases [4]. We note incidentally that we find it sufficient for our purposes to use the term ‘species’ in a generic sense, although one distinguishes in principle between elementary *components* and composite *species*.

of coupled, non-linear PDE's can be solved by a variety of numerical techniques. A common problem is the difficulty in establishing general criteria guaranteeing the *stability* of the numerical algorithms for solving systems of non-linear PDE's; these questions are handled on a case by case basis. Concerning the computer implementations of these solvers, the memory and time requirements present an extremely difficult task for practical two- and three-dimensional problems with present-day computers. As suggested in Ref. [5], algorithms that apply transport and chemical reactions sequentially appear to hold more promise. We have already seen that this iterative aspect is shared by our model.

The approach proposed in this work has been motivated by the following arguments:

- (a) We model physicochemical processes at a level intermediate between the *macroscopic level* described by PDE's and the *microscopic level* of molecular dynamics. The 'particles' of our model are mathematical abstractions of the actual molecules of various chemical species. The number of particles is large enough to make statistical concepts meaningful, but is still many orders of magnitude smaller than the real number of molecules involved. The CA is intended to describe macroscopic behaviour which does not depend on the details of the microscopic dynamics, but follows from general properties of the latter. The CA guarantees these essential properties by applying them directly to its elementary constituents, in a much more intuitive way than the continuum approach. For example, the constraints of mass and momentum conservation, together with some smoothness assumptions about the macroscopic variables, lead to the Navier-Stokes equations of fluid dynamics². Similarly, the diffusion equation follows essentially from the random nature of collisions at the microscopic level. The resulting computer code is simple and allows easy variation of the dynamics and the boundary conditions. Moreover, statistical fluctuations are inherently present in the CA, whereas PDE's rely on being able to define a physical quantity, e.g. particle density, as a continuous variable and thus neglect any local variations due to the microscopic nature of the process. This difference is crucial when the fluctuations have significant macroscopic consequences, as for example in

²Smoothness assumptions are indispensable for the derivation of macroscopic PDE's, such as the Navier-Stokes equations, from microscopic equations, such as the Boltzmann equation.

the reaction $a + b \rightarrow \textit{nothing}$ [20].

- (b) By working with *integers*, the CA simulation is free of *round-off errors*, which arise from the representation of real numbers by finite computer words and lead to possible instabilities of the numerical algorithms used to solve PDE's. This is a significant advantage when non-linear reaction terms are present, making the stability of PDE solvers hard to establish. All quantities in a CA simulation are intrinsically finite and infinities can only arise by extrapolation to some limit (e.g. infinite volume), in very much the way this is done with real systems [6]. The continuity required of the solutions of PDE's is, by contrast, physically inaccurate, as it presupposes an infinitesimal limiting procedure (e.g. averaging over a volume that shrinks to a point) which does not correspond to reality below a minimal scale (e.g. the volume per particle when evaluating particle density).
- (c) CA algorithms are naturally parallel, i.e. they process a large number of data simultaneously. This makes them suitable for massively parallel computers. In particular, the simple nature of the elementary physicochemical processes should allow simulation on massively parallel computers with relatively unsophisticated processors. Moreover, the local character of these processes implies that only a minimal amount of communication between physically neighbouring processors will be necessary. Computers with large numbers of processors (up to tens of thousands) operating in parallel and favouring next-neighbour communication are among those leading the push towards teraflop performance (10^{12} floating point operations per second) [7]. Supercomputers are also being used to solve PDE's with standard numerical methods, and the question arises if CA can provide a more efficient alternative (when fluctuation effects are uninteresting). In this respect, we note that the stochastic nature of the CA approach makes it in general slower than deterministic methods of solving PDE's, if the same time and space discretisation is used. On the other hand, these deterministic methods suffer invariably from stability problems, which can be overcome, but usually at great expense to the computation time. Here the CA approach has the important advantage that it is inherently stable. We there-

fore expect that the answer to the above question will depend highly on the specific application of interest.

The systems simulated in this work are conventionally described by reaction-transport equations of the form derived in Section 2 (Eq. (2.45)). As discussed above, these equations are based on several oversimplifying assumptions about the behaviour of real systems, but we shall use them here anyway as a reference point in testing our simulations. We justify this choice by the fact that reaction-transport PDE's lie invariably at the basis of all known models for the systems in which we are interested. We remain naturally open to the possibility that discrepancies between the CA approach and the solutions of the reaction-transport equations may arise from some element of microscopic reality (e.g. microscopic fluctuations) that the continuum approach fails to capture. This may lead to interesting corrections to the standard point of view. When no such corrections arise, the CA may be used to approximate the solutions of the continuum equations; it is of course essential to study how the result of the simulation converges to the continuous function it is approximating, as we refine the discretisation of space and time. The merits of the CA approach will then be judged in comparison with other numerical methods. *The aim of this work is to establish that the proposed CA can simulate a wide variety of physicochemical phenomena, ranging from simple annihilation reactions to complex autocatalytic reaction schemes leading to pattern formation. The discrete approach will be shown to be capable of approximating the solution of the reaction-transport PDE's. In some cases the results of the discrete and continuum approaches will disagree and in one of these the discrepancy will point to a fundamental shortcoming of the continuum approach.*

CA simulations are currently being performed by scientists in various disciplines, who seek in the simplicity of their elementary algorithms the unifying principles behind the often complex phenomena they observe [8]. Thus, fluid motion is being modelled via *lattice-gas automata* (LGA). Lattice-gas models have existed for several years and they were known to display certain hydrodynamic properties [9], but the recent increase in their popularity [10] has been largely brought about (i) by the advent of powerful supercomputers, and (ii) by the realisation that they can approximate hydrodynamic PDE's

[11]. LGA are special cases of deterministic CA. Our approach is more closely related with probabilistic LGA models of reaction-diffusion processes [12, 13]. All LGA models impose a limitation on the number of particles per lattice site, in the form of an *exclusion principle*. This is necessary when simulating CA on special purpose computers, which can support a small number of bits per site (e.g. CAM-6, [14]), and is useful for optimisation purposes on vector supercomputers. With computers becoming available that perform floating-point operations on many processors in parallel, we see no reason to maintain such a restriction, in particular since the enforced small number of particles per site severely limits the statistics of the simulation and makes either a bigger lattice or more simulations necessary. In addition, probabilistic models of diffusion with an exclusion principle are not able to model advection without introducing at the same time unwanted non-linearities [15]. In our model, by contrast, advection emerges naturally from the microscopic rule. An exclusion principle also makes it impossible to model local chemical reactions of arbitrary complexity. Increasingly complex reactions can be brought into our model with minor programming effort. Any model aiming at the description of the transport and chemistry of complex solute systems in geological media must be able to incorporate advection and arbitrary chemical reactions naturally. The model proposed here appears, in this light, most suitable for applications to systems of this kind.

The paper is organised as follows: In Section 2 the discrete model is introduced and the continuum limit is derived with special emphasis on the physical assumptions that lead to the desired continuum equations. Alternative microscopic rules and boundary conditions are also discussed. Extensive simulations of physicochemical systems and detailed comparisons with the corresponding differential equations are undertaken in Section 3. Discrepancies with the continuum approach will receive particular attention. Finally, in Section 4, we discuss computational feasibility, summarise our conclusions and set tasks for the future.

2 The Model

2.1 Time Evolution

Our aim in this section is to formulate a microscopic model for the time evolution of a system of particles moving randomly (with a possible bias in a given direction) and reacting chemically among themselves. The particles can be thought of as molecules in solution, migrating in a porous medium. The model will be general enough to simultaneously describe the diffusion and advection of several chemical species with different transport properties and subject to various chemical reactions.

In our model, space and time are discrete: particles reside on the sites of a regular lattice, with spacing λ , and the system evolves by a sequence of instantaneous transitions separated by time τ . In each transition, the system moves to a new state according to a local rule applied to all sites of the lattice, and the procedure is iterated in discrete time steps. Below, we shall define the local rule and proceed to show that, under certain conditions, the equations describing the time evolution of the discrete system go over to a set of differential equations in the limit $\lambda, \tau \rightarrow 0$.

We define an *evolution step* to consist of a *transport step* and a *chemical reaction step*. During the transport step, we consider each lattice site independently and, for each particle present, we make a random decision whether it will move or stay stationary, with probabilities chosen so as to obtain the desired macroscopic parameters. Having redistributed particles this way, we proceed to the chemical reaction step, in which we decide for each site independently whether the particles occupying it will react, with probabilities reflecting the macroscopic reaction rates. The reaction probability can be chosen according to a variety of rules, some of which may give rise to the same macroscopic behaviour. A minimal prerequisite for a reaction to take place is that there are sufficient particles of each reactant. For the reactions that do go ahead, we remove particles of the reactant species and add particles of the product species, according to the reaction equation. Having completed the chemical reaction step we proceed to the next evolution step and so on.

We begin the precise formulation of our model by considering a system of particles

belonging to various species s_α (for most purposes the index α will be used interchangeably with the name s_α of the species). The particles are located on the sites of a lattice \mathcal{L} . For simplicity, we consider a one-dimensional lattice. Extensions to higher dimensions are straightforward. We focus on a typical site at position x (we shall refer to it for brevity as ‘site x ’) in the interior of the lattice. At time t , there are $N_\alpha(x, t)$ particles of species α at x . We refer to $N_\alpha(x, t)$ as the occupation number. The values of $N_\alpha(x, t)$ for all species α and lattice sites x define the state of the system of particles at time t . We assume a given distribution, $N_\alpha(x, 0)$, of particles at $t = 0$, which provides the initial condition to our problem, and defer to a later point the discussion of boundary conditions. The evolution during a time step τ , from time t to $t + \tau$, amounts to applying on $N_\alpha(x, t)$ the product $\mathcal{C} \circ \mathcal{T}$ of the operators describing transport, \mathcal{T} , and chemical reactions, \mathcal{C} :

$$N_\alpha(x, t + \tau) = \mathcal{C} \circ \mathcal{T} N_\alpha(x, t). \quad (2.1)$$

The purpose of the transport operation is to move particles by one lattice spacing to the right with probability p , or to the left with probability q ($p + q \leq 1$). This is completed in two consecutive stages. Each stage consists of a local operation applied simultaneously to all lattice sites. Since the action of \mathcal{T} is defined for any set of occupation numbers, independent of a particular state of the system, we introduce a generic set of occupation numbers $\{\mathcal{N}_\alpha(x) : x \in \mathcal{L} - \partial\mathcal{L}\}$, where $\partial\mathcal{L}$ represents the lattice boundary. First, for every lattice site x and every species α , a random triplet $\boldsymbol{\xi}_{x,n} \equiv (\xi_{x,n}^{(-1)}, \xi_{x,n}^{(0)}, \xi_{x,n}^{(+1)})$ is drawn for each of the $\mathcal{N}_\alpha(x)$ particles of species α present at x ($n = 1, \dots, \mathcal{N}_\alpha(x)$). $\boldsymbol{\xi}_{x,n}$ takes one of the values $(1, 0, 0)$, $(0, 1, 0)$ or $(0, 0, 1)$ with probabilities p , $1 - p - q$ and q respectively. All $\boldsymbol{\xi}$ ’s are drawn anew at each update, but an explicit time index is omitted for simplicity. These triplets are stored for the second stage. We begin the second stage with a new, empty lattice and build the new occupation numbers according to

$$\mathcal{T}\mathcal{N}_\alpha(x) = \sum_{j=-1}^1 \sum_{n=1}^{\infty} \xi_{x+j\lambda,n}^{(j)} \theta(\mathcal{N}_\alpha(x + j\lambda) - n), \quad (2.2)$$

where j, n are integers and $\xi_{x+j\lambda,n}^{(-1)}, \xi_{x+j\lambda,n}^{(0)}, \xi_{x+j\lambda,n}^{(+1)}$ are the components of the random triplet $\boldsymbol{\xi}_{x+j\lambda,n}$. The θ -function is defined by $\theta(m) = 1$ for $m \geq 0$, and $\theta(m) = 0$ otherwise.

To show how the empty lattice is filled, we recall that $\mathcal{T}\mathcal{N}_\alpha(x) = 0$ at the beginning of the second stage. The site x is fed with particles from its *immediate neighbourhood*,

i.e. the sites preceding and following x , as well as the site itself (in 2 dimensions, the immediate neighbourhood of a site consists of 5 or 7 sites, for a square or triangular lattice respectively). On the RHS of Eq. (2.2), j runs over the sites of this neighbourhood, which are $x - \lambda, x$ and $x + \lambda$. For each one of these sites and for each particle present at the same site of the original lattice, we look up the corresponding random triplet stored previously. If the component $\xi_{x+j\lambda,n}^{(j)}$ is 1, one particle is added to $\mathcal{TN}_\alpha(x)$, if it is 0, $\mathcal{TN}_\alpha(x)$ is left unmodified. In physical terms this corresponds to particles moving to the right or left or remaining stationary with probabilities p, q and $1 - p - q$ respectively. The fact that one component of $\xi_{x,n}$ is always 1 and the rest 0 implies that the transport operation will place exactly one particle in the immediate neighbourhood of a site for each of the particles originally at that site, thus conserving particle number. Then Eq. (2.2), with $N_\alpha(x, t)$ substituted for $\mathcal{N}_\alpha(x)$, can be interpreted as yielding the number of particles of species α at x , after the transport phase of the update following time t : particles from the left (i.e. on site $x - \lambda$ at time t) move to x with probability p , particles from the right (i.e. on site $x + \lambda$ at time t) move to x with probability q and particles at x remain there with probability $1 - p - q$. The last probability can be related to a *retention factor* in the movement of the species α (see Section 3).

Next we define the chemical reaction operator \mathcal{C} using the equation:

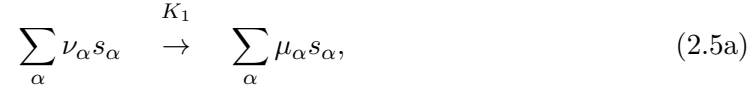
$$\mathcal{CN}_\alpha(x) = \mathcal{N}_\alpha(x) + \sum_{r=1}^R \left(\nu_{\alpha r}^{(f)} - \nu_{\alpha r}^{(i)} \right) \eta_{x,r}. \quad (2.3)$$

Here the summation runs over all chemical reactions in the problem at hand and $\eta_{x,r}$ is a Boolean random variable. $\nu_{\alpha r}^{(i)}$ and $\nu_{\alpha r}^{(f)}$ are the *stoichiometric coefficients* referring to initial and final species of the reaction r respectively. Naturally one can talk about ‘initial’ and ‘final’ species only if r is a one-way reaction. In fact, most of the reactions we expect to encounter are reversible, of the type



where K_1, K_2 are the *rate constants* and the stoichiometric coefficients $\nu_{\alpha}, \mu_{\alpha}$ are non-negative integers. The summations run over all species, but the stoichiometric coefficients vanish for species not involved in the reaction. It is convenient to express the above

reaction as two one-way reactions, namely



In Eq. (2.3) R is the total number of one-way reactions thus obtained and the index r runs over all such reactions (if there are irreversible reactions, they are added to the list as they are). Thus, if the first of the above two reactions occupies the r -th position on the list of one-way reactions, we identify ν_{α} and μ_{α} with $\nu_{\alpha r}^{(i)}$ and $\nu_{\alpha r}^{(f)}$ respectively. In Eq. (2.3) $\eta_{x,r}$ determines whether reaction r takes place ($\eta_{x,r} = 1$) or not ($\eta_{x,r} = 0$). In the latter case $\mathcal{N}_{\alpha}(x)$ is left unmodified (as far as reaction r is concerned), whereas in the former we subtract the number of reacting particles ($\nu_{\alpha r}^{(i)}$) and add the number of particles produced ($\nu_{\alpha r}^{(f)}$).

The probability with which $\eta_{x,r}$ is equal to 1 determines the rate at which reaction r takes place and should therefore be chosen to reflect the physical situation. In the physical case, a reaction rate depends both on the rate constant (K) and on the concentration (C_{α}) of reactants; thus for the reaction $a + 2b \rightarrow c$, the standard rate law gives the rate of production of c as the product $K C_a C_b^2$. Therefore, the probability of reaction has to depend on the rate constant and on the number of reactant particles available at the site of interest. Whereas we treat the rate constant as an intrinsic measurable property of the reaction, the functional dependence of the microscopic rule on occupation numbers ought to yield the concentration dependence of the standard rate law in the continuum limit. Thus, the probability that reaction r will take place at x (i.e. for $\eta_{x,r} = 1$) can be written as

$$\wp(\eta_{x,r} = 1 | \{\mathcal{N}_{\beta}(x) : s_{\beta} \in \mathcal{S}\}) \equiv P_r F_r(\{\mathcal{N}_{\beta}(x)\}), \quad (2.6)$$

where \mathcal{S} is the set of all species. P_r is a real number in the interval $[0, 1]$ and will be related to K_r later. F_r is a function of the occupation numbers and by varying it we can define various microscopic rules.

A simple choice for F_r is a function that ensures the presence of sufficient particles for the reaction to take place once at the microscopic level. One occurrence of reaction r means

that $\nu_{\alpha r}^{(i)}$ α -particles are subtracted and $\nu_{\alpha r}^{(f)}$ are added at the particular site. According to the rule defined with this F_r , *if there are sufficient reactant particles present, the reaction will take place at most once, with probability P_r* . Formally we define F_r as follows:

$$F_r(\{\mathcal{N}_\beta(x) : s_\beta \in \mathcal{S}\}) \equiv \prod_{\beta} \theta(\mathcal{N}_\beta(x) - \nu_{\beta r}^{(i)}) \quad (\text{Rule I}), \quad (2.7)$$

where the θ -function guarantees that sufficient particles are present and the product runs over all species. We recall the convention that $\nu_{\beta r}^{(i)} = 0$ if s_β is not a reactant in reaction r : if that is the case, the contribution of species β to the product is trivially equal to one, since all \mathcal{N}_β 's are non-negative, so that F_r depends effectively only on the occupation numbers of the species involved as reactants in reaction r .

According to the rule defined by Eq. (2.7), once there are sufficient reactant particles for a reaction to take place, the latter proceeds with a probability which does not further depend on the occupation numbers. Rule I leads to the standard rate law in the continuum limit, but only for low particle densities. On the other hand we expect that, the greater the number of particles present, the likelier should be the reaction. We introduce therefore another rule, in which the reaction probability is weighted by a product involving the number of particles of each species. We allow, namely, species β to contribute a factor $\prod_{m=1}^{\nu_{\beta r}^{(i)}} (\mathcal{N}_\beta(x) - m + 1)$ to F_r . *The principal motivation for this choice is that it leads to the standard rate law for any particle density*. Thus, the new rule amounts to defining

$$F_r(\{\mathcal{N}_\beta(x) : s_\beta \in \mathcal{S}\}) = \prod_{\beta} \prod_{m=1}^{\nu_{\beta r}^{(i)}} (\mathcal{N}_\beta(x) - m + 1) \quad (\text{Rule II}). \quad (2.8)$$

Here we allow the product to run over all species, with the convention $\prod_{m=1}^0 (\mathcal{N}_\beta(x) - m + 1) = 1$, which ensures that species β will contribute a factor 1 if it is not a reactant in reaction r ($\nu_{\beta r}^{(i)} = 0$).

Eqs. (2.1), (2.2), (2.3), (2.6) and (2.7) or (2.8) define the rule of evolution of the system of interacting particles. In the following subsections we are going to use these equations in order to derive discrete evolution equations, analogous to the finite difference equations (FDE's) approximating the differential reaction-transport equations. For this purpose we need to define a real-valued field, the *particle density* $\rho_\alpha(x, t)$, from the integer-valued occupation number $N_\alpha(x, t)$. It is clear of course that only $N_\alpha(x, t)$ is involved in the

simulation, whereas $\rho_\alpha(x, t)$ can be optionally defined at the level of the output and is not fed back into the simulation.

The occupation numbers obtained in a simulation of the discrete model possess a granularity which is not manifest in a typical measurement. Measured quantities are effectively averaged over a volume depending on the spatial resolution of the measuring apparatus. It is anyway clear that physical attributes of extended systems can only be defined after averaging over a certain minimal length scale. The continuum approach appears to describe physical quantities over arbitrarily short distances, but this becomes meaningless below the above minimal scale. Our approach lies closer to reality in that the transition from integers (occupation numbers) to real numbers (particle densities³) is effected via an averaging procedure. This can be performed either over a neighbourhood of lattice sites or over corresponding sites in an *ensemble* of states obtained by several independent simulations of the system. We make a *smoothness assumption*, according to which the particle density does not vary appreciably on the length scale of the neighbourhood used in the first of the above averaging procedures. The average densities of two such neighbourhoods may of course differ appreciably if their separation is on a larger scale. Under the smoothness assumption, the results of the above two averaging procedures should agree, within fluctuations. Based on this discussion, we define the particle density

$$\rho_\alpha(x, t) \equiv \langle N_\alpha(x, t) \rangle, \quad (2.9)$$

where $\langle \dots \rangle$ denotes an *ensemble average*.

2.2 Transport Equation

From a numerical point of view, transport differs from chemical reactions in two important respects: (i) The former involves communication of information between neighbouring sites; in the continuum limit this gives rise to derivative terms (advection, diffusion), which depend on the precise way the limit is taken. (ii) In our model, the evolution equations for pure transport are linear in the density and the respective FDE's are subject to well-defined stability criteria; this distinguishes them from the reaction-transport equations,

³We reserve the concept of *concentrations* for the physically measurable quantities, which will be obtained later by multiplying the *densities* by a scaling factor.

which are usually non-linear and follow no general stability criteria. For these reasons it will be worthwhile to concentrate first on pure transport. We begin, therefore, by replacing \mathcal{C} in Eq. (2.1) by the identity operator. Then the species propagate independently of each other and we can drop, for the purposes of the present derivation, the index α .

Combining Eqs. (2.9) and (2.1), the latter with $\mathcal{C} \equiv \mathbb{1}$, we obtain

$$\rho(x, t + \tau) = \langle N(x, t + \tau) \rangle = \langle \mathcal{T}N(x, t) \rangle. \quad (2.10)$$

According to Eq. (2.2),

$$\begin{aligned} \langle \mathcal{T}N(x, t) \rangle &= \sum_{n=1}^{\infty} \left(\langle \xi_{x-\lambda, n}^{(-1)} \rangle \langle \theta(N(x-\lambda, t) - n) \rangle + \langle \xi_{x, n}^{(0)} \rangle \langle \theta(N(x, t) - n) \rangle \right. \\ &\quad \left. + \langle \xi_{x+\lambda, n}^{(+1)} \rangle \langle \theta(N(x+\lambda, t) - n) \rangle \right) \\ &= p \langle N(x-\lambda, t) \rangle + (1-p-q) \langle N(x, t) \rangle + q \langle N(x+\lambda, t) \rangle \\ &= p\rho(x-\lambda, t) + (1-p-q)\rho(x, t) + q\rho(x+\lambda, t). \end{aligned} \quad (2.11)$$

Eq. (2.11) is exact and follows from the fact that the ξ 's are statistically independent of the N 's. In deriving (2.11) we made use of the expectation values of the components $\xi_{x, n}^{(j)}$:

$$\begin{pmatrix} \langle \xi_{x, n}^{(-1)} \rangle \\ \langle \xi_{x, n}^{(0)} \rangle \\ \langle \xi_{x, n}^{(+1)} \rangle \end{pmatrix} = \langle \xi_{x, n} \rangle = p \begin{pmatrix} 1 \\ 0 \\ 0 \end{pmatrix} + (1-p-q) \begin{pmatrix} 0 \\ 1 \\ 0 \end{pmatrix} + q \begin{pmatrix} 0 \\ 0 \\ 1 \end{pmatrix} = \begin{pmatrix} p \\ 1-p-q \\ q \end{pmatrix}, \quad (2.12)$$

as well as of the simple result

$$\begin{aligned} \sum_{n=1}^{\infty} \langle \theta(N(x, t) - n) \rangle &= \langle \sum_{n=1}^{\infty} \theta(N(x, t) - n) \rangle \\ &= \langle N(x, t) \rangle, \quad \forall x \in \mathcal{L}. \end{aligned} \quad (2.13)$$

The last equality follows from the fact that the θ -function contributes 1 to the sum for each value of n between 1 and $N(x, t)$ and 0 for higher values. We shall show the same result in a different way later (Eq. (2.29)).

From Eqs. (2.10) and (2.11) we deduce the evolution equation

$$\rho(x, t + \tau) = p\rho(x-\lambda, t) + (1-p-q)\rho(x, t) + q\rho(x+\lambda, t). \quad (2.14)$$

Eq. (2.14) can be readily rearranged as follows

$$\begin{aligned} \frac{\rho(x, t + \tau) - \rho(x, t)}{\tau} &= -V \frac{\rho(x+\lambda, t) - \rho(x-\lambda, t)}{2\lambda} + D \frac{\rho(x+\lambda, t) - 2\rho(x, t) + \rho(x-\lambda, t)}{\lambda^2}, \end{aligned} \quad (2.15)$$

where we have defined

$$V \equiv (p - q) \frac{\lambda}{\tau} \quad , \quad D \equiv (p + q) \frac{\lambda^2}{2\tau} \quad . \quad (2.16)$$

In Eq. (2.15) we recognise the forward difference approximation for the first time derivative and the central difference approximations for the first and second space derivatives of the density:

$$\begin{aligned} \frac{\rho(x, t + \tau) - \rho(x, t)}{\tau} &= \frac{\partial \rho(x, t)}{\partial t} + O(\tau), \\ \frac{\rho(x + \lambda, t) - \rho(x - \lambda, t)}{2\lambda} &= \frac{\partial \rho(x, t)}{\partial x} + O(\lambda^2), \\ \frac{\rho(x + \lambda, t) - 2\rho(x, t) + \rho(x - \lambda, t)}{\lambda^2} &= \frac{\partial^2 \rho(x, t)}{\partial x^2} + O(\lambda^2). \end{aligned} \quad (2.17)$$

Substituting these approximations in Eq. (2.15) we arrive at the equation

$$\frac{\partial \rho(x, t)}{\partial t} + O(\tau) = -V \frac{\partial \rho(x, t)}{\partial x} + D \frac{\partial^2 \rho(x, t)}{\partial x^2} + O(\lambda^2). \quad (2.18)$$

Taking the limit $\lambda \rightarrow 0$, $\tau \rightarrow 0$ and $p - q \rightarrow 0$ in such a way that λ^2/τ and $(p - q)\lambda/\tau$ remain finite, we obtain the transport equation

$$\frac{\partial \rho(x, t)}{\partial t} = -V \frac{\partial \rho(x, t)}{\partial x} + D \frac{\partial^2 \rho(x, t)}{\partial x^2} \quad . \quad (2.19)$$

On the RHS of Eq. (2.19) there is an advective term, with velocity V , and a diffusive/dispersive term, with *diffusion coefficient* D . We note that the continuum limit is taken in such a way that V and D , as defined in Eq. (2.16), remain finite. Eq. (2.15) is the forward-time centred-space finite difference approximation to the transport equation (2.19). We have thus shown that, *as far as pure transport is concerned, our model constitutes a stochastic way of solving the finite difference approximation to the continuum PDE.*

A few remarks are in order here:

- (a) The differential equation obtained in the continuum limit depends on the way the limit is approached. Let us first try to keep $p - q$ finite. We consider the migration of an ensemble of particles concentrated initially at the same lattice site. The density of particles evolves according to Eq. (2.15), whose RHS contains a term proportional to $p - q$ ('advection') and one proportional to $p + q$ ('diffusion'). After a finite time

$t \gg \tau$, diffusion would result in an average displacement $\sim \sqrt{\lambda^2(t/\tau)}$, whereas the particles would propagate a distance $\sim \lambda(t/\tau)$ in the same time due to advection. As $\lambda \rightarrow 0$ and $\tau \rightarrow 0$, but keeping λ/τ constant, an infinite number of updates (given by t/τ) would be needed to make the latter distance finite, but it is after an infinitely larger number of steps (given by $(t/\tau)^2$) that the former displacement would have a chance to become finite. In other words, diffusion would become infinitely slower than advection and the ensemble of particles would move without spreading. Thus, if we keep $p - q$ and λ/τ finite, then only the advective term survives as $\lambda, \tau \rightarrow 0$. If on the other hand one tries to keep $p - q$ and λ^2/τ finite, advection becomes infinitely fast and this particular limit is of no practical interest. The two processes will be comparable in the continuum limit, however, if $p - q$ vanishes like λ . $p - q$ is the bias in right/left displacement and gives the size of the advective velocity in units of lattice spacings per time step. By letting $p - q \rightarrow 0$ we curb the uncontrolled growth of the advective displacement, while preserving a finite average diffusive spread.

- (b) From the definitions of V and D and the obvious conditions $p - q \leq p + q \leq 1$, we deduce

$$V \frac{\tau}{\lambda} \leq 2D \frac{\tau}{\lambda^2} \leq 1 \quad . \quad (2.20)$$

In Eq. (2.20) we recognise the stability conditions for the FDE (2.15) [16, Eq. (5.1.18)]. These stability conditions are imposed by hand in the usual FDE approach to ensure that the round-off error introduced by numerical computation does not increase exponentially. Since we have shown the equivalence of our method to the FDE, it is not surprising that these inequalities hold, but it is an important feature of the random walk that they are implemented in an automatic and natural fashion.

- (c) If $p + q = 1$, the system is subject to the so-called ‘checkerboard parity’ [17]. Thus, if we colour sites in a checkerboard fashion, two particles occupying at one time sites of different colours will always be on differently coloured sites and will never meet. The system divides into two subsystems which alternate between sublattices of different colour, but remain forever decoupled. We shall show later in this section that, when particles are placed on a lattice according to a uniform random

distribution, the occupation numbers obey a Poisson distribution (Eq. (2.30)). The existence of two decoupled sublattices does not influence this result, as long as the particles are initially distributed evenly between the two sublattices. The opposite extreme would be to place all particles initially on sites of one sublattice and then perform a large number of diffusion steps. In that case, one of the two sublattices is alternately empty and the occupation numbers end up satisfying the Poisson distribution as if all particles were uniformly distributed only on the occupied sublattice: in Eq. (2.30) the density has to be doubled (or, equivalently, evaluated by dividing through half the number of lattice sites) and the probability for occupation number 0 has to be augmented by a probability of 1/2 that the site belongs to the empty sublattice. In intermediate cases, in which particles are placed with a bias favouring one sublattice, there will be a corresponding deviation from the Poisson distribution, if the latter is calculated on the assumption that particles are distributed over the entire lattice. The symmetry just described will obviously not hold if $p + q < 1$, i.e. if particles have a non-zero probability to remain stationary and thus populate the same sublattice on successive time steps. Checkerboard parity can also break down because of boundary conditions. Thus, the subsystems may mix if we impose periodic boundary conditions [12].

- (d) Species with different transport properties (advection velocity or diffusion coefficient) can be described on the same lattice by (i) moving particles belonging to different species by different numbers of lattice spacings at each update, or (ii) by moving species at different multiples of a time step. This way we can simulate, for instance, a problem of pure diffusion, where the diffusion coefficients of different species are in the ratio of integers. A more natural and physically appealing way to describe species with transport coefficients whose ratio may vary continuously is to make p and q species dependent. Given V_α and D_α , we evaluate p_α and q_α from the equations

$$p_\alpha = D_\alpha \frac{\tau}{\lambda^2} + \frac{V_\alpha \tau}{2 \lambda} \quad , \quad q_\alpha = D_\alpha \frac{\tau}{\lambda^2} - \frac{V_\alpha \tau}{2 \lambda} \quad . \quad (2.21)$$

If we choose τ and λ so that (i) $p_\alpha + q_\alpha = 1$ for the species with largest D_α ⁴ and (ii)

⁴In principle $p_\alpha + q_\alpha < 1$ for the species with largest D_α will do as well. This choice, however, slows

$|V_\alpha| \lambda / 2D_\alpha \leq 1$ for the species with largest $|V_\alpha| / D_\alpha$, then the conditions $p_\alpha \geq 0$, $q_\alpha \geq 0$ and $p_\alpha + q_\alpha \leq 1$ will be fulfilled for all species. Condition (i) determines τ as a function of λ and condition (ii) makes sure that λ is small enough to make the first term on the RHS of the equations (2.21) larger in absolute value than the second. We note in passing that one might think of treating cases with inhomogeneous transport parameters by making the probabilities position dependent. In that case the evolution equation (2.14) becomes

$$\rho(x, t + \tau) = p(x - \lambda)\rho(x - \lambda, t) + [1 - p(x) - q(x)]\rho(x, t) + q(x + \lambda)\rho(x + \lambda, t), \quad (2.22)$$

where p and q are functions of position and the species label need not be explicitly indicated. From Eq. (2.22) we readily derive the transport equation

$$\frac{\partial \rho(x, t)}{\partial t} = -\frac{\partial}{\partial x} [V(x)\rho(x, t)] + \frac{\partial^2}{\partial x^2} [D(x)\rho(x, t)], \quad (2.23)$$

where $V(x)$ and $D(x)$ are related to $p(x)$ and $q(x)$ according to Eq. (2.16). Note that Eq. (2.23) can be written in the more familiar form [4]

$$\frac{\partial \rho(x, t)}{\partial t} = -\frac{\partial}{\partial x} [W(x)\rho(x, t)] + \frac{\partial}{\partial x} \left[D(x) \frac{\partial \rho(x, t)}{\partial x} \right] \quad (2.24)$$

by defining $W(x) \equiv V(x) - dD(x)/dx$.

- (e) If we repeat the above derivation for a rectangular lattice in d dimensions, assuming the same coefficient of diffusion in all directions, we arrive at the result $D = P\lambda^2/2\tau d$, where P is the probability that a particle moves to another site during a transport step ($P = p + q$ in one dimension). P is a measure of particle mobility and is inversely proportional to the *retention factor* \mathcal{R} that will be introduced in Section 3, in connection with sorbing species.

2.3 Chemical Kinetics

We now consider the full problem in which an evolution step is completed by the action of the chemical reaction operator \mathcal{C} on the result of the transport operation. From Eqs.

 down the simulation and is not necessary, unless the value of τ has to be small for reasons such as those explained at the end of Subsection 2.3.

(2.1) and (2.3) we obtain:

$$\begin{aligned}
N_\alpha(x, t + \tau) &= \mathcal{C} \circ \mathcal{T}N_\alpha(x, t) \\
&= \mathcal{T}N_\alpha(x, t) + \sum_{r=1}^R \left(\nu_{\alpha r}^{(f)} - \nu_{\alpha r}^{(i)} \right) \eta_{x,r}
\end{aligned} \tag{2.25}$$

and

$$\begin{aligned}
\rho_\alpha(x, t + \tau) &= \langle N_\alpha(x, t + \tau) \rangle \\
&= \langle \mathcal{T}N_\alpha(x, t) \rangle + \sum_{r=1}^R \left(\nu_{\alpha r}^{(f)} - \nu_{\alpha r}^{(i)} \right) P_r \langle F_r(\{\mathcal{T}N_\beta(x, t) : s_\beta \in \mathcal{S}\}) \rangle,
\end{aligned} \tag{2.26}$$

where we have directly substituted for $\langle \eta_{x,r} \rangle$ the expression derived from Eq. (2.6).

At this point we need a specific ansatz for F_r in order to proceed further. Assuming the form given in (2.7) or (2.8), we are faced with the problem of taking the expectation value of a product of random variables. The simplest possibility is that these variables are *mutually independent*. This will be true if the occupation numbers of different species are mutually independent; in other words, if the number of particles of every species at a site is not correlated with the numbers of particles of the other species at that site. Correlations can arise as a consequence of interactions among the particles, i.e. collisions or reactions of all kinds. In our model, particles do not explicitly collide, but are scattered by a random background (we can think of each random scattering of a particle as simulating several collisions of a solute molecule with solvent or other solute molecules). Therefore, correlations can only arise as a result of chemical reactions. We shall see in Section 3 that correlations do occur in our model. We postulate, nevertheless, *molecular chaos*, i.e. the absence of correlations, for the purposes of our derivation and return to this point in the next section. Then the average of the product equals the product of the averages of the individual terms and we have to evaluate expressions of the type $\langle \theta(\mathcal{T}N_\alpha(x, t) - \nu_{\alpha r}^{(i)}) \rangle$ and $\langle \prod_{m=1}^{\nu_{\alpha r}^{(i)}} (\mathcal{T}N_\alpha(x, t) - m + 1) \rangle$, for rules I and II respectively.

We first derive the evolution equations using reaction rule I (Eq. (2.7)). By definition, $\theta(\mathcal{T}N_\alpha(x, t) - \nu_{\alpha r}^{(i)})$ is equal to 1 when there are not less than $\nu_{\alpha r}^{(i)}$ α -particles at site x after the transport operation and 0 otherwise. It follows that the ensemble average of the θ -function gives the fraction of ensemble members for which there are not less than $\nu_{\alpha r}^{(i)}$

α -particles at x . We define this fraction to be the probability that there are sufficient α -particles at that position:

$$\wp\left(\mathcal{T}N_\alpha(x, t) \geq \nu_{\alpha r}^{(i)}\right) \equiv \left\langle \theta\left(\mathcal{T}N_\alpha(x, t) - \nu_{\alpha r}^{(i)}\right) \right\rangle. \quad (2.27)$$

$\{N_\alpha(x, t) : s_\alpha \in \mathcal{S}\}$ is as much a set of occupation numbers as $\{\mathcal{T}N_\alpha(x, t) : s_\alpha \in \mathcal{S}\}$ and we can temporarily neglect \mathcal{T} :

$$\wp(N_\alpha(x, t) \geq n) \equiv \langle \theta(N_\alpha(x, t) - n) \rangle, \quad (2.28)$$

where n is any non-negative integer. It is easy to see that

$$\begin{aligned} \sum_{n=1}^{\infty} \wp(N_\alpha(x, t) \geq n) &= \sum_{n=1}^{\infty} \sum_{m=n}^{\infty} \wp(N_\alpha(x, t) = m) \\ &= \sum_{m=1}^{\infty} m \wp(N_\alpha(x, t) = m) \\ &= \langle N_\alpha(x, t) \rangle. \end{aligned} \quad (2.29)$$

We note that Eq. (2.13) follows from Eq. (2.29) and the definition (2.28).

We now need to relate the probability $\wp(N_\alpha(x, t) = n)$ to the density $\rho_\alpha(x, t)$. We are able to fulfill this task under the smoothness assumption, which guarantees that our definition of the density as an ensemble average (Eq. (2.9)) is equivalent to the alternative definition as a local spatial average. We employ, for the purpose of the present argument, the latter definition and recall that, according to the discussion above Eq. (2.9), local averages are evaluated over sections of the lattice which are inhabited by essentially homogeneous populations of particles. Following Ref. [1], let such a subsystem contain, at time t , N α -particles distributed evenly on M lattice sites. If site x belongs to the particular section of the lattice, then $\rho_\alpha(x, t) \simeq N/M$ and $\wp(N_\alpha(x, t) = n)$ can only depend on n and $\rho_\alpha(x, t)$. We wish to calculate the probability $\wp(N_\alpha(x, t) = n)$ that n particles (out of N) are found at x ($M, N \gg n$). There are $\binom{N}{n}$ ways of selecting n particles out of N . Once the n particles are placed at site x , the remaining $N - n$ particles can distribute themselves in $(M - 1)^{N-n}$ ways on the remaining $M - 1$ sites. Thus there is a total of $\binom{N}{n} (M - 1)^{N-n}$ configurations with n particles at x . The desired probability is obtained by dividing the number of these configurations by the number M^N of all possible

configurations of N particles on M sites:

$$\begin{aligned} \wp(N_\alpha(x, t) = n) &= \binom{N}{n} \frac{(M-1)^{N-n}}{M^N} = \frac{N!}{(N-n)! n!} \frac{(M-1)^{N-n}}{M^N} \\ &\simeq \frac{\rho_\alpha^n(x, t)}{n!} e^{-\rho_\alpha(x, t)} \quad \text{for } n \ll M, N \end{aligned} \quad (2.30)$$

which is just the Poisson distribution. Adopting, for convenience, the compact notation $\rho_\alpha(x, t + \tau/2) \equiv \langle \mathcal{T}N_\alpha(x, t) \rangle$, we write by analogy

$$\wp(\mathcal{T}N_\alpha(x, t) = n) \simeq \frac{\rho_\alpha^n(x, t + \tau/2)}{n!} e^{-\rho_\alpha(x, t + \tau/2)}. \quad (2.31)$$

No overdue significance should be attached to the fraction in the time argument $t + \tau/2$: it merely denotes an intermediate situation just before execution of the chemical reaction step.

Substituting the ansatz (2.7) in Eq. (2.26), applying the factorisation of the expectation value that follows from the molecular chaos hypothesis, employing the definition (2.27) and finally assuming an equality for Eq. (2.31), we find

$$\begin{aligned} \rho_\alpha(x, t + \tau) &= \rho_\alpha(x, t + \tau/2) + \sum_{r=1}^R \left(\nu_{\alpha r}^{(f)} - \nu_{\alpha r}^{(i)} \right) P_r \prod_{\beta} \wp \left(\mathcal{T}N_\beta(x, t) \geq \nu_{\beta r}^{(i)} \right) \\ &= \rho_\alpha(x, t + \tau/2) + \sum_{r=1}^R \left(\nu_{\alpha r}^{(f)} - \nu_{\alpha r}^{(i)} \right) P_r \prod_{\beta} \sum_{n=\nu_{\beta r}^{(i)}}^{\infty} \wp(\mathcal{T}N_\beta(x, t) = n) \\ &= \rho_\alpha(x, t + \tau/2) + \sum_{r=1}^R \left(\nu_{\alpha r}^{(f)} - \nu_{\alpha r}^{(i)} \right) P_r \prod_{\beta} \sum_{n=\nu_{\beta r}^{(i)}}^{\infty} \frac{\rho_\beta^n(x, t + \tau/2)}{n!} e^{-\rho_\beta(x, t + \tau/2)}, \end{aligned} \quad (2.32)$$

where

$$\rho_\alpha(x, t + \tau/2) = p_\alpha \rho_\alpha(x - \lambda, t) + (1 - p_\alpha - q_\alpha) \rho_\alpha(x, t) + q_\alpha \rho_\alpha(x + \lambda, t). \quad (2.33)$$

Rearranging terms as in Eq. (2.15) we deduce from Eqs. (2.32) and (2.33)

$$\begin{aligned} &\frac{\rho_\alpha(x, t + \tau) - \rho_\alpha(x, t)}{\tau} \\ &= -V_\alpha \frac{\rho_\alpha(x + \lambda, t) - \rho_\alpha(x - \lambda, t)}{2\lambda} + D_\alpha \frac{\rho_\alpha(x + \lambda, t) - 2\rho_\alpha(x, t) + \rho_\alpha(x - \lambda, t)}{\lambda^2} \\ &\quad + \sum_{r=1}^R \left(\nu_{\alpha r}^{(f)} - \nu_{\alpha r}^{(i)} \right) k_r \prod_{\beta} \sum_{n=\nu_{\beta r}^{(i)}}^{\infty} \frac{\nu_{\beta r}^{(i)!}}{n!} \rho_\beta^n(x, t + \tau/2) e^{-\rho_\beta(x, t + \tau/2)}, \end{aligned} \quad (2.34)$$

where

$$V_\alpha \equiv (p_\alpha - q_\alpha) \frac{\lambda}{\tau}, \quad , \quad D_\alpha \equiv (p_\alpha + q_\alpha) \frac{\lambda^2}{2\tau} \quad (2.35)$$

and the rate constant k_r is defined as

$$k_r \equiv \frac{P_r}{\tau} \frac{1}{\prod_{\alpha} \nu_{\alpha r}^{(i)}} \quad (\text{Rule I}). \quad (2.36)$$

k_r should not be confused with the physical rate constant K_r which will be defined shortly.

This is as far as we can go with the discrete model. We now wish to derive the continuum limit of the full model. With the continuum approximations (2.17), Eq. (2.34) becomes

$$\begin{aligned} \frac{\partial \rho_{\alpha}(x, t)}{\partial t} + O(\tau) &= -V_{\alpha} \frac{\partial \rho_{\alpha}(x, t)}{\partial x} + D_{\alpha} \frac{\partial^2 \rho_{\alpha}(x, t)}{\partial x^2} + O(\lambda^2) \\ &+ \sum_{r=1}^R \left(\nu_{\alpha r}^{(f)} - \nu_{\alpha r}^{(i)} \right) k_r \prod_{\beta} \sum_{n=\nu_{\beta r}^{(i)}}^{\infty} \frac{\nu_{\beta r}^{(i)}!}{n!} \rho_{\beta}^n(x, t) e^{-\rho_{\beta}(x, t)} + O(\tau). \end{aligned} \quad (2.37)$$

In Subsection 2.2 we let λ, τ and $p_{\alpha} - q_{\alpha} \rightarrow 0$, while keeping λ^2/τ and $(p_{\alpha} - q_{\alpha})\lambda/\tau$ finite. In the presence of chemical reactions, we also take $P_r \rightarrow 0$, but keep P_r/τ finite for all r . It follows immediately that $p_{\alpha} - q_{\alpha}$ and P_r are $O(\lambda)$ and $O(\tau)$ respectively. Taking the continuum limit of Eq. (2.37) as described, we derive the reaction-transport equation

$$\frac{\partial \rho_{\alpha}(x, t)}{\partial t} = -V_{\alpha} \frac{\partial \rho_{\alpha}(x, t)}{\partial x} + D_{\alpha} \frac{\partial^2 \rho_{\alpha}(x, t)}{\partial x^2} + \sum_{r=1}^R \left(\nu_{\alpha r}^{(f)} - \nu_{\alpha r}^{(i)} \right) k_r \prod_{\beta} \sum_{n=\nu_{\beta r}^{(i)}}^{\infty} \frac{\nu_{\beta r}^{(i)}!}{n!} \rho_{\beta}^n(x, t) e^{-\rho_{\beta}(x, t)} \quad (\text{Rule I}). \quad (2.38)$$

We note that the forward-time centred-space FDE corresponding to Eq. (2.38) is similar but not identical to the discrete evolution equation (2.34). The difference lies in the time at which ρ_{β} is evaluated: for the FDE one uses the value of ρ_{β} at time t , while for the evolution equation ρ_{β} is evaluated at the end of the transport step performed at t . Moreover, iteration of Eq. (2.34) involves a two-step process where $\rho_{\beta}(x, t + \tau/2)$ is first generated through Eq. (2.33).

To obtain the standard form of the rate terms we have to consider low particle densities ($\rho_{\alpha} \ll 1$). If the latter are sufficiently low, then the sums in Eq. (2.38) are dominated by the lowest-order terms and we obtain products of the type $\prod_{\beta} \rho_{\beta}^{\nu_{\beta r}^{(i)}}$:

$$\frac{\partial \rho_{\alpha}(x, t)}{\partial t} \simeq -V_{\alpha} \frac{\partial \rho_{\alpha}(x, t)}{\partial x} + D_{\alpha} \frac{\partial^2 \rho_{\alpha}(x, t)}{\partial x^2} + \sum_{r=1}^R \left(\nu_{\alpha r}^{(f)} - \nu_{\alpha r}^{(i)} \right) k_r \prod_{\beta} \rho_{\beta}^{\nu_{\beta r}^{(i)}}(x, t). \quad (2.39)$$

Eq. (2.39) is typical of the kind of equations numerically solved by conventional approaches. It is therefore desirable that the discrete model reduce to a set of such equations

in some limit, under well-defined assumptions. If that is the case, it is sensible to test simulations of the discrete model by making sure that their predictions converge to the solutions of the appropriate differential equations. The chemical reaction rule defined by Eqs. (2.3), (2.6) and (2.7) leads to Eq. (2.39) only for low particle densities. As we shall demonstrate in Section 3, this restriction to low densities severely limits the efficiency of simulations that use Rule I.

We now employ rule II and show that it leads to the standard reaction-transport equations independent of particle density. We substitute Eq. (2.8) in Eq. (2.26) and calculate the expectation value of $F_r(\{\mathcal{T}N_\beta(x,t) : s_\beta \in \mathcal{S}\})$. If we assume, as before, molecular chaos, the expectation value of the product over β factorises. If we further invoke the smoothness assumption and the Poisson distribution which this implies (Eq. (2.31)), then the individual terms of the product have the form

$$\begin{aligned}
\langle \prod_{m=1}^{\nu_{\alpha r}^{(i)}} (\mathcal{T}N_\alpha(x,t) - m + 1) \rangle &= \sum_{n=0}^{\infty} \prod_{m=1}^{\nu_{\alpha r}^{(i)}} (n - m + 1) \wp(\mathcal{T}N_\alpha(x,t) = n) \\
&= \sum_{n=\nu_{\alpha r}^{(i)}}^{\infty} \prod_{m=1}^{\nu_{\alpha r}^{(i)}} (n - m + 1) \frac{\rho_\alpha^n(x, t + \tau/2)}{n!} e^{-\rho_\alpha(x, t + \tau/2)} \\
&= \sum_{n=\nu_{\alpha r}^{(i)}}^{\infty} \frac{\rho_\alpha^n(x, t + \tau/2)}{(n - \nu_{\alpha r}^{(i)})!} e^{-\rho_\alpha(x, t + \tau/2)} \\
&= \rho_\alpha^{\nu_{\alpha r}^{(i)}} \left(x, t + \frac{\tau}{2} \right) e^{-\rho_\alpha(x, t + \tau/2)} \sum_{n=\nu_{\alpha r}^{(i)}}^{\infty} \frac{\rho_\alpha^{n - \nu_{\alpha r}^{(i)}}(x, t + \tau/2)}{(n - \nu_{\alpha r}^{(i)})!} \\
&= \rho_\alpha^{\nu_{\alpha r}^{(i)}} \left(x, t + \frac{\tau}{2} \right) e^{-\rho_\alpha(x, t + \tau/2)} \sum_{n=0}^{\infty} \frac{\rho_\alpha^n(x, t + \tau/2)}{n!} \\
&= \rho_\alpha^{\nu_{\alpha r}^{(i)}} \left(x, t + \frac{\tau}{2} \right). \tag{2.40}
\end{aligned}$$

On the RHS of the first equality above, the summation over n need only be carried out from $n = \nu_{\alpha r}^{(i)}$, because the product over m always vanishes for $0 \leq n \leq \nu_{\alpha r}^{(i)} - 1$. Repeating the steps of our earlier derivation of the continuum limit, we arrive at (cf. Eq. (2.38))

$$\frac{\partial \rho_\alpha(x,t)}{\partial t} = -V_\alpha \frac{\partial \rho_\alpha(x,t)}{\partial x} + D_\alpha \frac{\partial^2 \rho_\alpha(x,t)}{\partial x^2} + \sum_{r=1}^R \left(\nu_{\alpha r}^{(f)} - \nu_{\alpha r}^{(i)} \right) k_r \prod_{\beta} \rho_\beta^{\nu_{\beta r}^{(i)}}(x,t) \quad (\text{Rule II}), \tag{2.41}$$

where

$$k_r = P_r / \tau \quad (\text{Rule II}). \tag{2.42}$$

Eq. (2.41) holds as a strict equality without the additional assumption of low density.

If ρ_α were solute concentrations, this would be the form commonly used in modelling systems with transport and chemical reactions. We have already remarked that particle densities are not the same as measurable concentrations. Clearly, we do not expect in the foreseeable future to be able to treat particle numbers comparable to Avogadro's number. We therefore assume that it is legitimate to work with numbers of particles that are by orders of magnitude smaller than Avogadro's number and obtain the respective concentrations $C_\alpha(x, t)$ by rescaling the densities $\rho_\alpha(x, t)$:

$$C_\alpha(x, t) \equiv \gamma \rho_\alpha(x, t). \quad (2.43)$$

We further assume that the scaling factor γ is universal (i.e. independent of species, space, time and the value of the density itself). Thus, we typically fix the value of γ from the initial conditions of the simulation (total particle density) and the real problem it purports to model (total concentration). We then perform the simulation and recover the concentrations at the desired times and locations by multiplying the densities at those times and locations by γ . If we substitute $\rho_\alpha = C_\alpha/\gamma$ into Eq. (2.41), we can absorb γ in the rate constants by defining the new rate constants K_r :

$$K_r \equiv k_r \gamma^{-\sum_\alpha \nu_{\alpha r}^{(i)} + 1}. \quad (2.44)$$

Then, the concentrations satisfy equations of the standard form:

$$\frac{\partial C_\alpha(x, t)}{\partial t} = -V_\alpha \frac{\partial C_\alpha(x, t)}{\partial x} + D_\alpha \frac{\partial^2 C_\alpha(x, t)}{\partial x^2} + \sum_{r=1}^R \left(\nu_{\alpha r}^{(f)} - \nu_{\alpha r}^{(i)} \right) K_r \prod_\beta C_\beta^{\nu_{\beta r}^{(i)}}(x, t). \quad (2.45)$$

Here the parameters V_α, D_α and K_r model directly properties of the physical system. In particular, K_r is identified with the physical rate constants in Eq. (2.4). We note that, if we substitute $\rho_\alpha = C_\alpha/\gamma$ into Eq. (2.38), then γ cancels out if only linear terms (transport terms and, possibly, linear reactions) are present, but in general non-linear terms result in a non-trivial γ -dependence. For low densities, rule I yields Eq. (2.45) in an approximate form, following from Eq. (2.39).

It should be mentioned that even rule II is not completely free of limitations on the density. The reason is quite different this time and becomes obvious if one substitutes (2.8) in Eq. (2.6). Since the probability for $\eta_{x,r} = 1$ must be ≤ 1 (we refer to this condition as *probability conservation*), the product of P_r and the appropriate combination

of occupation numbers at any site should not exceed one. For example, if r is the reaction $a + 2b \rightarrow c$, we should have $P_r N_a N_b (N_b - 1) \leq 1$. One has to make sure, therefore, that particle density is low enough to guarantee that the probability for the above product to exceed one is negligibly small. Alternatively, since it is the ratio P_r/τ that is related to physical parameters, we can handle arbitrarily high particle densities by making P_r and, consequently, τ appropriately small. The limit in this case is set by the resulting increase in the number of iterations and the accordingly greater computation time.

In Section 3 we shall study in detail a reaction-diffusion system in which particles of the species a , b and c interact via the reversible reaction



The reaction-transport equation for the concentration of species a is obtained as a special case of Eq. (2.45):

$$\frac{\partial C_a(x, t)}{\partial t} = -V_a \frac{\partial C_a(x, t)}{\partial x} + D_a \frac{\partial^2 C_a(x, t)}{\partial x^2} - K_1 C_a(x, t) C_b(x, t) + K_2 C_c(x, t). \quad (2.47)$$

According to Eqs. (2.36) and (2.44), if there is at least one a - and one b -particle at a site, the reaction $a + b \rightarrow c$ will occur with probability $P_1 = \tau \gamma K_1$. Similarly, if there is at least one c -particle, it will disintegrate into an a and a b with probability $P_2 = \tau K_2$. If we are in a diffusion-limited regime, where chemical equilibrium is attained on a much shorter time scale than that of diffusion, then a dynamic equilibrium is established locally between the reactions $a + b \rightarrow c$ and $c \rightarrow a + b$, the two rates cancelling each other in Eq. (2.47):

$$K_1 C_a C_b = K_2 C_c \rightarrow \frac{C_c}{C_a C_b} = \frac{K_1}{K_2} \rightarrow \frac{\rho_c}{\rho_a \rho_b} = \frac{k_1}{k_2}, \quad (2.48)$$

where we have omitted for simplicity the space and time arguments. Eq. (2.48) is a special case of the *law of mass action* for ideal solutes, with *equilibrium constant* $\mathcal{K} = K_1/K_2$.⁵

If we use rule I, the exact reaction-transport equations are obtained as a special case of (2.38), for example,

$$\frac{\partial \rho_a(x, t)}{\partial t} = -V_a \frac{\partial \rho_a(x, t)}{\partial x} + D_a \frac{\partial^2 \rho_a(x, t)}{\partial x^2} - k_1 \left(1 - e^{-\rho_a(x, t)}\right) \left(1 - e^{-\rho_b(x, t)}\right) + k_2 \left(1 - e^{-\rho_c(x, t)}\right), \quad (2.49)$$

⁵The law of mass action in this simple form holds only for infinite dilution. For higher concentrations, interactions among the species (e.g. of electrostatic nature) complicate the situation. Such effects may in principle be incorporated in our model, but are not considered in its present form.

where $k_1 = \gamma K_1$ and $k_2 = K_2$. We note that no low density assumption has been made here. According to (2.49), the law of mass action (Eq. (2.48)) is replaced by

$$\frac{1 - e^{-\rho_c}}{(1 - e^{-\rho_a})(1 - e^{-\rho_b})} = \frac{k_1}{k_2} . \quad (2.50)$$

For $\rho_a, \rho_b, \rho_c \ll 1$ we recover the familiar law of mass action and, if we write $C_a(x, t) \equiv \gamma \rho_a(x, t)$ etc., Eq. (2.49) reduces to (2.47) as an approximate equation; if we are sufficiently close to chemical equilibrium, $K_1 C_a C_b = \gamma k_1 \rho_a \rho_b$ is of the same order of magnitude as $K_2 C_c = \gamma k_2 \rho_c$ and we can say that Eq. (2.47) holds to $O(C_c^2/\gamma^2) = O(\rho_c^2)$.

2.4 Homogeneous System

In a homogeneous system, the particle density is independent of the spatial variable and we can write it as $\rho_\alpha(t)$. We define $\rho_\alpha(t)$ as the average number of α -particles per site:

$$\rho_\alpha(t) \equiv \frac{\sum_x N_\alpha(x, t)}{\mathcal{V}} , \quad (2.51)$$

where $\sum_x N_\alpha(x, t)$ is the total number of particles of species α and \mathcal{V} is the total number of sites. In two dimensions, with N_x sites in the x -direction and N_y sites in the y -direction, $\mathcal{V} \equiv N_x \times N_y$. For a homogeneous system, this definition is equivalent to the ensemble average used in Section 2.

We repeat the steps that led from Eq. (2.25) to Eqs. (2.38) and (2.41), but with $\langle \dots \rangle$ understood this time as the *average over all sites*. The first term on the RHS of Eq. (2.25) becomes $\langle \mathcal{T} N_\alpha(x, y, t) \rangle = \rho_\alpha(t) = \langle N_\alpha(x, t) \rangle$ upon averaging, as if the transport operator \mathcal{T} had not been applied at all to the occupation number. This is natural, as transport does not change the average properties of a homogeneous system. We factorise the expectation value of F_r in Eq. (2.26) under the assumption of molecular chaos (see the discussion following Eq. (2.26)) and evaluate the individual terms using the Poisson distribution (derived on the basis of the arguments that led to Eq. (2.30), but applied this time to the system as a whole). We thus arrive at an equation for $\rho_\alpha(t)$:

$$\frac{d\rho_\alpha(t)}{dt} = \sum_{r=1}^R \left(\nu_{\alpha r}^{(f)} - \nu_{\alpha r}^{(i)} \right) k_r \prod_{\beta} \sum_{n=\nu_{\beta r}^{(i)}}^{\infty} \frac{\nu_{\beta r}^{(i)}!}{n!} \rho_{\beta}^n(t) e^{-\rho_\alpha(t)} \quad (\text{Rule I}), \quad (2.52a)$$

$$\frac{d\rho_\alpha(t)}{dt} = \sum_{r=1}^R \left(\nu_{\alpha r}^{(f)} - \nu_{\alpha r}^{(i)} \right) k_r \prod_{\beta} \rho_{\beta}^{\nu_{\beta r}^{(i)}}(t) \quad (\text{Rule II}). \quad (2.52b)$$

2.5 Boundary Conditions

We shall discuss here the transport behaviour of particles when they reach the lattice boundary. Since chemical reactions will not enter in the present discussion, we shall make use only of Eq. (2.10). Each boundary condition will be determined once we formulate the microscopic transport rule which replaces Eq. (2.2) for sites at the lattice boundary.

We first consider an *impermeable boundary*, with particles bouncing back when they reach it. In one dimension we can set the boundary at the first site on the left (say, $x = 0$) and the last on the right ($x = x_{max}$). We consider the left end of the lattice. The first two sites are $x = 0$ and $x = \lambda$ respectively. We define the transport operation as before by the rule: $\xi_{x,n} = (1, 0, 0)$, $(0, 1, 0)$ or $(0, 0, 1)$ with probability p , $1 - p - q$ and q respectively, unless $x = 0$, in which case $\xi_{x,n} = (1, 0, 0)$ or $(0, 1, 0)$ with probability p and $1 - p$ respectively (p and q are the same as in the interior of the lattice). In other words, once a particle reaches the left boundary, it moves to the right with the same probability p as in the interior of the lattice and remains at the boundary with probability $1 - p$. Equivalently, one may think of the boundary as lying at $-\lambda/2$ with particles at $x = 0$ moving according to the same rule as in the interior, but bouncing back to $x = 0$ within the same transport step if they hit the boundary. The equivalent of Eq. (2.11) for $x = 0$ is obtained from the above probabilities and the fact that there are no particles coming from the left:

$$\rho(0, t + \tau) \equiv \langle \mathcal{T}N(0, t) \rangle = (1 - p)\rho(0, t) + q\rho(\lambda, t), \quad (2.53)$$

Eq. (2.53) can be rearranged as follows

$$\begin{aligned} \frac{\rho(0, t + \tau) - \rho(0, t)}{\tau} &= \frac{q\rho(\lambda, t) - p\rho(0, t)}{\tau} \\ &= \frac{\lambda}{\tau} \left\{ (p + q) \frac{\rho(\lambda, t) - \rho(0, t)}{2\lambda} - \frac{p - q}{2\lambda} [\rho(\lambda, t) + \rho(0, t)] \right\}. \end{aligned} \quad (2.54)$$

In the limit $\lambda, \tau \rightarrow 0$, with $p - q \sim O(\lambda)$ and $\lambda^2/\tau \sim O(1)$, the LHS of Eq. (2.54) remains finite while on the RHS $\lambda/\tau \rightarrow \infty$. This implies that the expression in the curly brackets

on the RHS vanishes so that

$$\frac{\rho(\lambda, t) - \rho(0, t)}{\lambda} = \frac{p - q}{(p + q)\lambda} [\rho(\lambda, t) + \rho(0, t)] = \frac{V}{2D} [\rho(\lambda, t) + \rho(0, t)], \quad (2.55)$$

where we have used the definitions (2.16). In the continuum limit we obtain

$$\left[V\rho(x, t) - D\frac{\partial\rho(x, t)}{\partial x} \right] \Big|_{x=0} = 0 . \quad (2.56)$$

Eq. (2.56) is a statement of the condition that the *total flux* of solute (i.e. the sum of the *advective flux* $V\rho(x, t)$ and the *diffusive/dispersive flux* $-D\partial\rho(x, t)/\partial x$) vanishes at $x = 0$. This is intuitively clear from the definition of the impermeable boundary: any particles that reach it bounce off so that there is no flux across the boundary.

It is common in solute transport problems to specify either the concentration or its gradient at the boundary. These or mixed boundary conditions (i.e. relating the concentration with its gradient, such as Eq. (2.56)) can be easily implemented in our simulations once their physical background is clear. Thus, in the case when the concentration at the $x = 0$ boundary is fixed, it may be assumed that there is a large homogeneous reservoir, extending beyond the system of interest and having the given concentration. Introducing explicitly a reservoir beyond the boundary at $x = 0$ would be correct but impractical. This situation can be more efficiently simulated by assigning to $x = 0$ at each transport step an occupation number from a set of random numbers obeying the appropriate Poisson distribution (instead of applying the simulation rule at $x = 0$). A special case is that of a sink, i.e. vanishing concentration, at $x = 0$. The occupation number is then set at all times equal to zero at $x = 0$ and the evolution rule is applied normally to all sites of the lattice interior.

Alternatively, one may specify $\partial\rho(x, t)/\partial x|_{x=0} = 0$ as the boundary condition. To simulate this, we add formally site $x = -\lambda$ to the lattice. Before each transport step we set the occupation number at $x = -\lambda$ by $N(-\lambda, t) = N(\lambda, t)$. The evolution rule is then applied to all other lattice sites, including $x = 0$:

$$\begin{aligned} \rho(0, t + \tau) &= p\rho(-\lambda, t) + (1 - p - q)\rho(0, t) + q\rho(\lambda, t) \\ &= p\rho(\lambda, t) + (1 - p - q)\rho(0, t) + q\rho(\lambda, t) \end{aligned} \quad (2.57)$$

which can be rearranged as

$$\frac{\rho(0, t + \tau) - \rho(0, t)}{\tau} = (p + q) \frac{\rho(\lambda, t) - \rho(0, t)}{\tau}. \quad (2.58)$$

Arguing as before, we must have $\rho(\lambda, t) - \rho(0, t) \sim O(\lambda^2)$, if the RHS of (2.58) is to remain finite in the continuum limit. It follows that $\partial\rho(x, t)/\partial x|_{x=0} = [\rho(\lambda, t) - \rho(0, t)]/\lambda + O(\lambda) \rightarrow 0$, as $\lambda \rightarrow 0$. In physical terms, we make the diffusive flux vanish at the boundary by superposing equal and opposite amounts of outgoing and incoming diffusive flux; this leaves only advection to take care of net solute transport across the boundary.

A *periodic boundary condition* is often computationally convenient and is used when the precise behaviour of the boundary layer is not important, e.g. with translationally invariant homogeneous systems or when the boundary is too far away to influence the region of interest. We impose a periodic boundary condition by connecting the two ends of the lattice, so that particles crossing the right boundary appear automatically on the left boundary and particles crossing the left boundary appear on the right boundary.

3 Simulation of reaction-transport processes

The model formulated in Section 2 is very general and can describe a wide variety of coupled transport-chemical reaction processes. In this section our primary aim is to demonstrate the versatility of the model by using it to simulate various systems. After demonstrating a simple system undergoing both diffusion and advection, we concentrate on systems of diffusing particles subject to various chemical reaction schemes. A thorough discussion is given of the reactions $a + b \rightleftharpoons c$ and $a + b \rightarrow c$; these reactions are particularly suitable for displaying the essential microscopic aspects of the simulation. In each case, the results of the simulations are compared with the ones obtained from the corresponding PDE's ⁶. The purpose of the comparison is to test the validity of the smoothness and molecular chaos assumptions used to derive the PDE's in Section 2, as well as to study how the simulation converges to the continuum result. Lastly, we show that our model is also capable of simulating complex autocatalytic reaction-diffusion systems which, under non-equilibrium conditions, display remarkable spatial and temporal structures.

3.1 Diffusion and Advection

We first discuss solute transport without chemical reactions. Advection and diffusion arise as the macroscopic result of a random walk. In fact, from a microscopic point of view, there is no fundamental difference between the two processes. If the random walk is unbiased (equal probability of motion in all directions) there is only diffusion and no advection, whereas a bias in favour of a certain direction produces diffusion coupled with advection in the chosen direction. Fig. 1 shows the result of a simulation of solute transport on a one-dimensional lattice. We simulate simultaneously two solutes with advection velocities $V_1 = 0.5 m/y$ and $V_2 = V_1/10$ and diffusion coefficients $D_1 = 25 m^2/y$ and $D_2 = D_1/10$. ⁷ Taking $\tau = 10^{-3} y$ and $p_1 + q_1 = 1$, we use the second of Eqs. (2.16) to determine λ . The probabilities p_1 , q_1 , as well as p_2 , q_2 , are calculated from Eq. (2.21).

⁶The differential equations are solved using standard finite difference methods. We do not intend to discuss here the convergence of the standard methods. All results obtained with them have been checked for convergence and are indistinguishable for our purposes from the true solutions of the continuum equations.

⁷The second solute can be thought of as being retarded by a factor $\mathcal{R} = 10$ due to sorption on the surface of the solid matrix. If one assumes instantaneous sorption equilibrium and a linear relationship between liquid and solid phase concentrations, the effect of sorption can indeed be reduced to a retention factor \mathcal{R} that divides the transport coefficients V_α and D_α .

Figure 1: Result of one-dimensional simulation (species 1: solid circles, species 2: open circles) compared with the solution of the transport equation (species 1: solid curve, species 2: dashed curve) at $t = 240y$. Parameters and initial conditions are given in the text.

Initially both concentrations are equal to 1 (arbitrary units) for $x \leq 0$, and 0 for $x > 0$. The simulation begins with 200 particles of each species per site to the left of $x = 0$ and the concentration is calculated by averaging the occupation number over cells of 100 lattice sites and normalising by a factor $\gamma = 1/200$. The boundary condition is uninteresting here, because the boundary is chosen far enough, so that its influence does not reach the displayed region by the time considered. In the figure, the solution of the transport equation (2.19) is shown for comparison. Error bars of length equal to one standard deviation were estimated and were always found to be smaller than the plotting symbol. The small fluctuations around the solid curve are of statistical nature and diminish if we increase the number of particles used in the simulation.

3.2 $\mathbf{a + b \rightleftharpoons c}$, homogeneous case

We introduce chemical reactions by looking first at a system of particles which is initially homogeneous. We begin the simulation by placing particles on a two-dimensional lattice according to a uniform random distribution. As we saw in Section 2, for a homogeneous system the spatial derivatives of the density vanish and the reaction-transport equations (2.38) and (2.41), corresponding to reaction rules I and II respectively, reduce to

the chemical rate equations (2.52a) and (2.52b), which describe the evolution of uniform particle densities. It is important to note that these equations have been derived under the assumption of molecular chaos. In reality, correlations between particles and density fluctuations do occur, and on occasion, notably in some irreversible reactions as well as in some autocatalytic systems maintained far from equilibrium, lead to inhomogeneities, even for systems which initially are homogeneous. Later we shall discuss such reaction schemes; then of course, the average particle density need not follow Eqs. (2.52a) and (2.52b). For the moment, however, we consider the case where the system remains homogeneous as a function of time, and we address the question of how microscopic dynamics drives a discrete system towards equilibrium.

(a) Reaction rule I

We consider a homogeneous system of a -, b - and c -particles reacting via the reversible reaction $a + b \rightleftharpoons c$. At each time step every particle moves randomly to one of the four nearest sites. Particles react according to rule I: if there are at least one a - and one b -particle at a site, then, with probability P_1 , one a - and one b -particle are removed and a c -particle is added; whereas, if there are one or more c -particles at a site, then one of them is replaced by an a - and a b -particle with probability P_2 . As long as we discuss homogeneous systems, we shall average densities over the whole lattice and express them only as functions of time, $\rho_\alpha(t)$ (cf. Subsection 2.4). We follow the approach to equilibrium by looking at the time evolution of the *reaction quotient* $\rho_c(t)/\rho_a(t)\rho_b(t)$.

Let $p_{\alpha x}$ ($q_{\alpha x}$) be the probability that an α -particle moves by one lattice spacing λ to the right (left) along the x -direction and $p_{\alpha y}$ ($q_{\alpha y}$) the probability that it moves up (down) by the same distance along the y -direction in one transport step. Assuming all species to have the same diffusion coefficients, we take $p_{\alpha x} + q_{\alpha x} + p_{\alpha y} + q_{\alpha y} = 1$, $\forall \alpha$, i.e. particles always move to a neighbouring site.

Here, as in all cases below, we consider the case of no advection for convenience; when necessary, advection can be easily included in our model as demonstrated in Subsection 3.1 above. Thus we set $V_{\alpha x} \equiv (p_{\alpha x} - q_{\alpha x})\lambda/\tau = 0$ and $V_{\alpha y} \equiv (p_{\alpha y} - q_{\alpha y})\lambda/\tau = 0$, where $V_{\alpha x}$ and $V_{\alpha y}$ are the advection velocities in the x - and y -directions respectively (thus $p_{\alpha x} = q_{\alpha x}$ and

$p_{\alpha y} = q_{\alpha y}, \forall \alpha$). We further assume equal diffusion coefficients in the x - and y -directions ($D_{\alpha x} \equiv (p_{\alpha x} + q_{\alpha x})\lambda^2/2\tau = D_{\alpha y} \equiv (p_{\alpha y} + q_{\alpha y})\lambda^2/2\tau$). Putting together the constraints on the various displacement probabilities, we deduce $p_{\alpha x} = q_{\alpha x} = p_{\alpha y} = q_{\alpha y} = 1/4$ and $D_{\alpha x} = D_{\alpha y} = \lambda^2/4\tau \equiv D$. For convenience, these conditions will hold for all two-dimensional systems in this paper. We begin the simulation with 50 000 particles of each species on a two-dimensional lattice of 500×500 sites (i.e. a density of 0.2 particles of each species per site) with periodic boundary conditions. The reaction probabilities are determined through the relations $k_r = P_r/\tau$, where the rate constants are taken to be $k_1 = 0.8$ and $k_2 = 0.2$.

For our initial simulation we take $\tau = 1$ (arbitrary units) and examine the time development of the reaction-diffusion system up to time $t = 20$. In Fig. 2a the solid circles denote the mean value of the reaction quotient for an ensemble of 21 systems. The estimated error bars are smaller than the plotting symbol. The solid curve is obtained by solving the rate equations (2.52a). According to the latter, the reaction quotient reaches the equilibrium value 3.50 at roughly $t = 10$ and remains constant thereafter. This value can also be derived by solving Eq. (2.50) subject to the constraints $\rho_a(t) - \rho_b(t) = \text{constant}$ and $\rho_a(t) + \rho_c(t) = \text{constant}$, which obviously hold for $a + b \rightleftharpoons c$. The result of the simulations evolves instead towards a slightly higher equilibrium value and then runs parallel to the solid curve. *The simulations lead to an equilibrium state with relatively more c -particles than predicted by the rate equations.*

That the discrete result does not agree with the exact solution of the rate equations is due to two reasons. As far as the rate equation is concerned, the problem is completely specified by the initial conditions, the rate constants k_r , and the final time of interest, $t = 20$. Apparently, the time discretisation used in the simulation is too coarse to provide agreement with these rate equations. To illustrate this, we solve the coupled FDE's obtained from Eqs. (2.52a) with the same time step, $\tau = 1$, as used in the simulations⁸. The result of the FDE's (dashed line in Fig. 2a) lies far from the exact result it is approximating (showing that the time discretisation is not sufficient); but it also lies far from the result of the simulations (although the latter use the same time discretisation as the

⁸The FDE's are obtained by substituting $[\rho_\alpha(t + \tau) - \rho_\alpha(t)]/\tau$ for $d\rho_\alpha(t)/dt$ in (2.52a).

Figure 2a: Time dependence of the reaction quotient for a two-dimensional, homogeneous system of a -, b - and c -particles, reacting via $a + b \rightleftharpoons c$ according to rule I: mean value over 21 simulations with $\tau = 1$ (solid circles), exact result of differential rate equations (solid curve) and approximate result of FDE's (dashed curve). Also shown is the result of 21 simulations with $\tau = 1/5$ (open circles). The values of the transport and reaction parameters, as well as the initial conditions, are given in the text.

Figure 2b: The same as Fig. 2a, but with 10 d.p.r.

FDE's).

The discrepancy between the simulations and the solution of the FDE's is of a different origin and can be understood as follows: The rate equations and the approximating FDE's rely on the assumption that a - and b -particles are uncorrelated. In the simulations, this assumption does not hold. At the rate of one diffusion step per reaction step (d.p.r.), the a - and b -particles originating from the disintegration of a c -particle remain sufficiently close to each other for the probability of their meeting again (with a subsequent chance of reaction) to be significantly higher than in a uniform distribution of particles, i.e. if the assumption of molecular chaos were valid. The reverse reaction, $c \rightarrow a + b$, is not affected by correlations. As a result, $a + b \rightarrow c$ is enhanced with respect to $c \rightarrow a + b$ and relatively more c -particles are produced, resulting in a higher reaction quotient. The conditions of molecular chaos can be systematically approached by performing an increasing number, n_D , of d.p.r. In each evolution step of our simulation, we repeat the transport operation n_D times before we perform the reaction operation once. This multiplies the diffusion coefficient by a factor n_D in the continuum limit, but, for a homogeneous system, the rate equations remain the same. The reaction quotient in the asymptotic state is shown in Fig. 3 for $n_D = 1, 2, 3, 5$ and 10. To obtain the value for $n_D = \infty$, we replace the transport operation by a random redistribution of particles⁹. We see that, *as increased diffusion washes out correlations between the particles, the equilibrium reaction quotient approaches the value obtained from the rate equations*. Similar conclusions concerning correlation effects have been drawn in Ref. [18].

The time evolution of the reaction quotient for $n_D = 10$ is shown in Fig. 2b (solid circles). As expected from the preceding paragraph, correlations play a much lesser rôle and the system reaches a steady state only slightly higher than that predicted by the rate equations. However, for times $t \leq 5$, there is a serious discrepancy with the exact solution of the rate equations. Comparing again with the solution of the FDE's (dashed curve), we find good agreement, thus confirming the smallness of residual correlations. In fact, the agreement becomes perfect if we redistribute particles randomly between reaction steps

⁹We have tested the validity of this identification by letting a system of particles diffuse from different initial distributions. After sufficient iterations of our diffusion algorithm, the occupation number obeys essentially the Poisson distribution over the accessible lattice sites, as expected from a uniform random distribution of particles.

Figure 3: Reaction quotient for the system of Fig. 2a, averaged over 9000 time steps in the steady state of a simulation, for different numbers of diffusion steps per reaction step.

($n_D = \infty$).

We now look at the way our discrete model approaches the continuum limit. As we refine the time step, we expect to obtain the exact prediction of the rate equations, in very much the way the solution of an FDE converges to the exact solution. We perform simulations with a shorter time step $\tau = 1/5$. Then we also have to scale down the reaction probabilities P_1 and P_2 by a factor 5, in order to obtain the same rate constants k_1 and k_2 . The results of the simulations executed with these parameters are shown as open circles in Fig. 2a ($n_D = 1$) and in Fig. 2b ($n_D = 10$). The reaction quotient is here averaged over 21 independent simulations and statistical errors are smaller than the plotting symbol.

The finer discretisation obviously leads to better agreement with the exact result in both Figs. 2a and 2b. In the case of Fig. 2b, where correlations are almost absent, the improvement over the previous set of simulations (solid circles) is attributable to the use of a smaller time step, in the sense of convergent FDE schemes. In the case of Fig. 2a, however, the finer discretisation improves the agreement also partly by reducing indirectly the effect of correlations. This can be seen as follows: As the reaction probabilities P_r decrease (by the same factor, say m , as the time step), particles react more weakly in a

single update. This is compensated by exactly that many more updates within a given time span, so that the overall reaction strength (rate constant) remains intact. The particles execute, however, m times more movements to neighbouring sites in a given time span. As a result of this increased agility, particles originating at the same site are more inclined to lose memory of their common origin and correlations are subsequently weakened. In fact, *as the continuum limit is approached, any correlations between the a - and b -particles will disappear.*

Using reaction rule I (Eq. (2.52a)), we obtain a reaction quotient of 3.50 at chemical equilibrium, for the particular parameters chosen. The standard rate law, Eq. (2.52b), leads to a significantly different value of $k_1/k_2 = 4.00$. This difference is obtained for an initial particle density of 0.2. It is clear that the particle density has to be significantly lower than 0.2, if we intend to reproduce the standard law by using Rule I. In fact a density of 0.005 would be necessary to reduce the discrepancy at equilibrium below 1%. For low particle densities the statistics is poor for each individual simulation and one has to perform many of them or use a bigger lattice. On the other hand, one can also obtain better statistics if higher particle densities can be used. We therefore proceed to investigate reaction rule II, which allows us to use higher densities.

(b) Reaction rule II

We first apply rule II to a system of particles with the same initial density, 0.2, as with rule I. Fig. 4a shows the result of 21 simulations, on a 500×500 lattice, of a homogeneous system of a -, b - and c -particles diffusing with $n_D = 1$ and reacting via $a + b \rightleftharpoons c$, according to rule II. Transport and kinetic parameters, as well as initial and boundary conditions, are identical with those of the previous simulations on such a lattice. The time step is taken to be $\tau = 1/10$ and the reaction parameters $P_1 = 0.08$ and $P_2 = 0.02$. According to rule II, if there are n_a a -particles and n_b b -particles at a site, then one a - and one b -particle are removed and a c -particle is added with probability $P_1 n_a n_b$, whereas, if there are n_c c -particles, one of them is replaced by an a - and a b -particle with probability $P_2 n_c$. A smaller time step is dictated by the need to make P_1 and P_2 sufficiently small so that the

Figure 4a: Time dependence of the reaction quotient for a two-dimensional, homogeneous system of a -, b - and c -particles, reacting via $a + b \rightleftharpoons c$ according to rule II: mean value over 21 simulations (open circles) and exact result of differential rate equations (solid curve).

Figure 4b: The same as Fig. 4a, but with an initial density of 1 and appropriate rescaling of parameters and densities as explained in the text.

probability conservation conditions (cf. Eqs. (2.6) and (2.8))

$$\wp(\eta_{x,1} = 1 | \{N_\alpha(x, t) = n_\alpha\}) = P_1 n_a n_b \leq 1 \quad (3.1a)$$

$$\text{and } \wp(\eta_{x,2} = 1 | \{N_\alpha(x, t) = n_\alpha\}) = P_2 n_c \leq 1. \quad (3.1b)$$

will be respected in all but an insignificant number of cases. For $P_1 = 0.08$, condition (3.1a) is violated if $n_a n_b > 12$. Assuming a Poisson distribution for the occupation numbers, we readily estimate that $n_a n_b > 12$ occurs at an arbitrary site with probability 0.8×10^{-8} [2]. From this we also estimate that there is a 0.2% likelihood that probability conservation will be violated at all (i.e. anywhere on the lattice) in one iteration step. This likelihood is negligible for practical simulations and, in the rare cases when the probability of reaction does exceed one, we can safely set this probability equal to one. Due to the substantially smaller time spacing ($\tau = 1/10$), correlation effects are insignificant even for 1 d.p.r. in this case.

Moving to a higher particle density, we simulate, on a 200×200 lattice, a homogeneous system of a -, b - and c -particles, reacting via $a + b \rightleftharpoons c$, with an initial density of 1 particle of each species per site and periodic boundary conditions. The time step is $\tau = 1/10$, as in the last set of simulations, and we perform 1 d.p.r. To obtain the same rate equations and initial conditions as before (and hence the same continuum result to compare with), we have to first rescale the previous value of P_1 by a factor $\gamma = 0.2$ (leaving P_2 intact), then perform the simulation and finally multiply the resulting densities by the same factor. The scaling factor γ is a dimensionless version of the factor used to relate particle density to concentration in Section 2. The result of 21 simulations is shown in Fig. 4b. In this case, probability conservation is violated if $n_a n_b > 62$, which occurs with probability 0.3×10^{-9} at a given site and with probability 0.1×10^{-4} anywhere on the lattice during an iteration step.

(c) Optimisation of Rule II

We have seen that rule I approximates the standard rate law only for sufficiently low particle densities. Under this constraint, the quality of statistics can be improved either by performing more simulations, or by increasing the number of lattice sites. Rule II,

however, leads to the standard rate law without the restriction of low particle densities and, in that case, better statistics can also be achieved by utilising the higher densities. On the other hand, rule I is simpler and its simulation computationally more efficient for a given density. It is very important to assess whether the additional freedom (wider density range) afforded by rule II can be exploited in order to obtain higher computational efficiency (for the same statistics). More precisely, we address the questions: (i) whether there is an optimal density which minimises the computation time needed to perform a simulation using rule II, (ii) how this computation time compares with the time required by rule I. We shall not attempt to provide a universal answer to these questions; instead, we concentrate on the example of $a + b \rightleftharpoons c$ we have been considering so far, emphasising the conclusions that have wider validity.

We perform a series of simulations of the above system of a -, b - and c -particles on a 200×200 lattice, using rule II and different values of the initial particle density, which we take to be the same for all species: $\rho_a(0) = \rho_b(0) = \rho_c(0) \equiv \rho$. The reaction parameters P_r are rescaled each time so that the continuum rate equations and initial conditions are the same as those in the last set of simulations above. We finally rescale the densities $\rho_\alpha(t)$ obtained from the simulation by the ratio of the reference density 0.2 to the initial density of particles on the lattice, ρ , thus $\rho_\alpha(t) \longrightarrow \tilde{\rho}_\alpha(t) \equiv (0.2/\rho)\rho_\alpha(t)$. In each case we calculate the reaction quotient $\tilde{\rho}_c(t)/\tilde{\rho}_a(t)\tilde{\rho}_b(t)$ and compare its asymptotic value with the result obtained by solving Eq. (2.52b) with $k_1 = 0.8$, $k_2 = 0.2$, $\rho = 0.2$ and the stoichiometric coefficients appropriate for $a + b \rightleftharpoons c$.

We have already seen that the result of the simulations lies arbitrarily close to that of the rate equations for the right choice of τ . Here we require that the result of the simulations does not deviate by more than $\sim 10 - 15\%$ from the exact result. This is roughly the discrepancy we obtain if we solve Eq. (2.52a) with the same parameters (resulting in a reaction quotient of 3.50 instead of 4.00, as given by the standard rate law). This discrepancy reflects the systematic error expected from rule I, since the densities calculated with that rule converge to values that satisfy Eq. (2.50) instead of the standard Eq. (2.48).

Given the above maximum acceptable error, we seek to minimise the computation

Figure 5: (a) Normalised minimum computation time for one simulation, as a function of initial particle density: Rule II (crosses, curve to guide the eye) and rule I (solid circle). (b) Estimated minimum computation time ($T_c = c/\rho P_1$), corresponding to a 15% likelihood of probability-conservation violation at a site, as a function of particle density, with c fitted to actual T_c at $\rho = 10$.

time by reducing the number of iteration steps. This is equivalent to increasing τ , which in turn implies a larger P_1 (of course, also a larger P_2 , but this has no influence on most of our considerations). Increasing τ can have a number of possible effects on the results of the simulation. Firstly, we expect deviation from the rate equation in the sense that the corresponding FDE deviates from the rate equation. However, it can be easily checked that the FDE gives the same reaction quotient at equilibrium as the rate equation, independently of the value of τ . Since we have chosen to use only this asymptotic ratio for comparison of simulations, increasing τ will not give rise to such numerical convergence problems in our case. On the other hand, an increase in the probability of reactions leads to stronger correlations between the particles, and this does affect the reaction quotient at equilibrium. By varying the number of diffusion steps per reaction step, we have actually found that the effect of such correlations is relatively small. We find instead that the main effect of increasing τ , and hence P_1 , is that probability conservation is violated more frequently. Since an unphysical probability (> 1) is treated in our simulation as if it were 1, the reaction $a + b \rightarrow c$ is partly suppressed each time P_1 exceeds 1. This amounts to

a suppression of the production of c -particles and appears macroscopically as a reduction of the reaction quotient.

For a given initial density ρ , we obtain our minimum computation time, $t_c(\rho)$, when the reaction quotient is reduced by the maximum amount allowed, namely by the factor 10 – 15% discussed above. For all densities we normalise this minimum computation time by demanding the same statistics as for $\rho = 0.2$; thus we introduce the normalised minimum computation time $T_c(\rho)$ by the equation $T_c(\rho) = \gamma t_c(\rho)$, where $\gamma = 0.2/\rho$. In Fig. 5a we show T_c as a function of the initial density ρ : there is a minimum for ρ between 3 and 5. Thus, *there is a range of densities for which rule II can be simulated with maximum efficiency*. To compare this with the efficiency of rule I, we also show the computation time for a simulation of that rule, performed with initial density 0.2 and the same number of iteration steps as the optimal simulation of rule II with the same density. We see that, *although rule I may be significantly more efficient than rule II for the same density, it can be less efficient than rule II when the latter is used with a higher density*. In other words, using rule II with higher densities can offer an advantage in computational efficiency (in the particular case we are considering, by a factor of 4-5).

In Fig. 5a we do not continue to higher densities because probability conservation begins to be violated due to the size of P_2 and the picture becomes more complex beyond $\rho \simeq 10$. We expect however that the upward trend of the curve in Fig. 5a continues to higher densities. To show that higher densities result in ever increasing computation times we argue as follows: It is plausible to assume that, for high particle densities ρ , the computation time T_c required for given statistics is roughly proportional to $N_s \times N_t \times N_p$, where N_p is the total number of particles, N_t the number of iteration steps in a single simulation and N_s the number of independent simulations required to achieve the desired statistics. Since $N_s \propto 1/\rho$ and $N_p \sim \rho N_x^2$ (assuming a rectangular $N_x \times N_y$ lattice, with N_x of the same order of magnitude as N_y), we have $T_c \propto N_x^2 \times N_t$. But $N_x = L/\lambda$ and $N_t = T/\tau$, where L is the linear size of the system and T the time interval during which the system evolves. For a reaction of the type $a + b \rightarrow c$, we saw below Eq. (2.47) that $\tau = P_1/\gamma K_1$, where γ relates ρ to the physical concentration C : $C = \gamma\rho$ (cf. Eq. (2.43)); from Eq. (2.16) we also find $\lambda \propto \sqrt{D\tau}$. Putting things together, we deduce $T_c \propto 1/(\rho P_1)^2$.

Since our aim is to minimise computation time, P_1 has to be as high as possible, with the upper bound set by the maximum acceptable likelihood of probability-conservation violation. Given the density, we can calculate the violation probability for any given value of P_1 assuming a Poisson distribution of the occupation numbers. Conversely, if we fix the violation probability, we can determine the corresponding value of P_1 . To be definite, let us set the violation probability at a site to be 15%. It is then found that P_1 decreases, as a function of ρ , faster than $1/\rho$, which implies that $1/(\rho P_1)^2$, and hence T_c , is an increasing function of ρ . The decrease of P_1 , and hence of τ and λ , with ρ results in an increase of lattice size and iteration number which in turn implies an increase in computation time. There is a subtle point in the above argument which deserves mentioning. For a homogeneous system we need not require a fixed diffusion coefficient D and hence we can keep λ and N_x fixed while we vary P_1 and τ . This is in fact what we did in the the simulations described above. Then $T_c \propto N_t \propto 1/\rho P_1$, which is shown in Fig. 5b, is also an increasing function of ρ . We conclude that there is no advantage in increasing the density beyond the minimum in Fig. 5a.

3.3 $a + b \rightarrow c$, homogeneous case

An interesting situation arises when we turn off the reverse reaction. Then the problem consists of a - and b -particles that diffuse and combine to form inert c -particles upon meeting. Equivalently, we may neglect species c altogether and think in terms of an annihilation reaction between ‘particles’ a and ‘antiparticles’ b .

We assume the numbers of a - and b -particles to be initially equal ($\rho_a(0) = \rho_b(0) \equiv \rho$), which implies that they will remain so. Then, the density $\rho_a(t) = \rho_b(t)$ obeys the rate equation $d\rho_a/dt = -k\rho_a^2$, where $k \equiv P_1/\tau$ is the rate constant of the reaction $a + b \rightarrow c$ (of course $P_2 = 0$). The solution of the rate equation is $\rho_a(t) = \rho/(1 + k\rho t)$, which behaves asymptotically in time as t^{-1} . It is known, however, that, in microscopic simulations, the long-time behaviour of the system is determined by long-range density fluctuations, which give rise to an asymptotic $t^{-1/2}$ behaviour in two dimensions. Following Ref. [20], this can be understood as follows: Initially ($t = 0$), particles a and b are distributed randomly with uniform probability. At a much later time t , particles have spread over a length

scale $\ell_D \equiv (Dt)^{1/2}$ due to diffusion and fluctuations on a longer length scale have not had time to dissolve. In a two-dimensional region of linear size ℓ_D , there are initially on the order of $\rho\ell_D^2$ particles of each species; however, due to statistical fluctuations, there will be deviations from this number. Assuming variations of one standard deviation, one can expect the difference between the numbers of a - and b -particles to be of order $(\rho\ell_D^2)^{1/2}$. Therefore, in this region of volume $\sim \ell_D^2$, there is an excess density of a - or b -particles on the order of $\rho^{1/2}/\ell_D$. For a given rate constant k , we can always choose the time t large enough so that the bulk of the particles will have annihilated and only the excess density will remain by that time. Thus, what remains of the initial system are regions occupied by one or the other species, with density of order $\ell_D^{-1} \sim t^{-1/2}$; the reaction takes place only along the boundaries of these regions and is slower than under the well-mixed conditions assumed by the rate equation. Thus, *the initial fluctuations in particle density give rise to a decay mechanism which is slower than t^{-1} and dominates at sufficiently long times. The rate equation, by neglecting fluctuations, does not account for this mechanism and predicts the wrong long-time behaviour.*

Simulations using our model reproduce asymptotically this result. At finite times, we observe that the deviation from the result of the rate equations depends on the details of the experiment: (i) it decreases when the diffusion constant increases, since this limits the range of contributing fluctuations, and (ii) it increases with the rate constant, as the bulk of the particles annihilate faster and clusters develop sooner (Fig. 6, where $\tau = 1$).

3.4 $a + b \rightleftharpoons c$, at an interface

Moving away from homogeneous systems, we consider a system of a - and b -particles which initially ($t = 0$) occupy the $x \geq 0$ and $x \leq 0$ halves of a two-dimensional ($N_x \times N_y$) lattice respectively. For $t > 0$, they diffuse and react, producing c -particles ($a + b \rightarrow c$); the latter diffuse and disintegrate into a - and b -particles ($c \rightarrow a + b$). In the process, the a - and b -particles diffuse into the regions of each other, while c -particles form a distribution peaked at $x = 0$. Here and in what follows, reaction rule II is used. We perform simulations, in which there are initially 50 000 particles on each half of a 500×500 lattice (i.e. 0.4 particles/site) and other parameters are the same as before. Since the

Figure 6: Average density of a two-dimensional, homogeneous system reacting via $a+b \rightarrow c$ according to rule II, as a function of time, for different values of the rate constant: simulation (solid curves) compared with rate equation (dotted curves).

Figure 7: Width of reaction zone and of distribution of annihilation events for a two-dimensional, initially separated system reacting via $a+b \rightarrow c$ according to rule II, as a function of time: solution of reaction-transport equations (dotted, dashed and dot-dashed curves for 1, 4 and 10 d.p.r. respectively) compared with simulation (solid curves).

macroscopic problem is effectively one-dimensional for the particular initial condition, we define particle density as a function of time and the spatial variable x only, by averaging over the occupation number along the y -direction:

$$\rho_\alpha(x, t) \equiv \frac{1}{N_y} \sum_y N_\alpha(x, y, t) \quad . \quad (3.2)$$

We wish to express quantitatively the size of the reaction front, i.e. the region around $x = 0$ where reactions take place. This is obviously related to the spatial overlap of the densities of reacting particles. As a - and b -particles spread on the lattice, their overlap steadily increases¹⁰. Using $\rho_\alpha(x, t)$, we define the *width of the reaction zone*, w , as the standard deviation of the product of the a - and b -particle distributions:

$$\bar{x}(t) = \frac{1}{N_x} \sum_x x \rho_a(x, t) \rho_b(x, t) \quad , \quad w^2(t) = \frac{1}{N_x} \sum_x [x - \bar{x}(t)]^2 \rho_a(x, t) \rho_b(x, t) \quad . \quad (3.3)$$

The width obtained from these simulations is consistent, within statistical fluctuations, with the asymptotic time dependence, namely $t^{1/2}$, predicted by the reaction-diffusion equations. This behaviour is understood if we note that our choice of parameter values corresponds to a diffusion-limited regime. Then, particles essentially spread according to the $t^{1/2}$ law expected from pure diffusion, with the relative abundance of different species determined locally by chemical equilibrium. If the reaction probabilities are much smaller than 1, then the time dependence of w displays more variety at times short on the time scale of the reactions, but the asymptotic behaviour remains the same [21].

3.5 $a + b \rightarrow c$, at an interface

We now turn off the reverse reaction, as in the homogeneous case above, keeping all other parameters unchanged. In the diffusion-limited regime, a - b annihilation around $x = 0$ proceeds so fast that new particles do not have the time to get there by diffusion. As a result, a *depletion zone* develops around $x = 0$, where the densities of a - and b -particles are significantly smaller than their initial values. The width of this zone grows as $t^{1/2}$. It can be shown from the reaction-diffusion equations that the width of the reaction zone, as defined previously, varies asymptotically with time as $t^{1/6}$ [22]. For reasons that

¹⁰We always choose the size of the system so that the overlap does not reach the boundary during the simulation; the precise boundary condition is, therefore, irrelevant for the present discussion.

will become clear shortly, we define alternatively the *width of the spatial distribution of annihilation events up to time t* . Each time an a - and a b -particle annihilate, we keep a record of the event and then we count at each lattice site all events that took place up to time t . The distribution of annihilation events is identical with the distribution of c -particles, provided the latter remain permanently at the site where they are produced. The new width, w' , is then defined by replacing in (3.3) the product of the a - and b -densities by the density of the inert, immobile c -species. It can be easily shown that w' behaves asymptotically also as $t^{1/6}$ according to the reaction-diffusion equations.

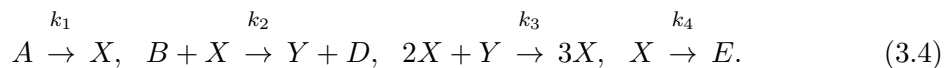
In Fig. 7 we compare the result of the simulation (solid curves) with that of the reaction-diffusion equations: the dotted curves describe the time evolution of the widths of the reaction zone (w , upper curve) and the distribution of reaction events (w' , lower curve) for 1 d.p.r., while the dashed and dot-dashed curves describe the same quantities for 4 and 10 d.p.r. respectively. The comparison is clearly facilitated by the better statistics in the case of w' . We notice that for 1 d.p.r. the result of the simulation lies above that of the reaction-diffusion equations; moreover, the former apparently grows with a higher time exponent than the expected $1/6$. This is consistent with Ref. [13]. It is clear that, with enhanced diffusion (4 and 10 d.p.r.), the result of the simulation converges systematically to that of the continuum equations. Continuing the simulation to greater times modifies slightly the time exponents, which depend further on the dimensionality of the lattice [23] and the reaction strength, but the following qualitative picture remains: *in the absence of sufficient diffusive mixing, a and b annihilate less strongly and hence penetrate deeper into the regions of each other, resulting in a bigger additional widening of the reaction zone.* This slowing down of the annihilation process is probably due to the inability of diffusion to destroy fluctuations beyond a certain length scale, as in the homogeneous case above. The analogy cannot be upheld, however, beyond the length scale set by the size of the depletion zone, which is absent in the homogeneous system.

3.6 Complex reaction-diffusion systems

We now consider reaction-diffusion systems which are significantly more complex than the ones considered so far. They involve species with different transport properties (e.g.

diffusion coefficients) and various chemical reactions, some of which are autocatalytic, i.e. they require the presence of a certain species in order to produce more of it. Autocatalytic reactions play an important rôle in biological processes. Systems subject to autocatalytic reactions can undergo phase transitions far from thermodynamic equilibrium. A system can be kept far from chemical equilibrium, for example, by suppressing reverse reactions and/or by an external supply of reactants. In such systems, the (unique) steady state, which is stable near equilibrium, may become unstable as certain parameters are varied. Then a phase transition to a new state may take place. Thus, an originally homogeneous state may become unstable and spatial concentration patterns (Turing structures) may develop spontaneously (see e.g. [24, 25]). A crucial element in the formation of Turing structures is a significant difference in the diffusion coefficients of two species; the faster species, the *inhibitor*, hinders by chemical action the spreading of the slower one, the *activator*, and the latter accumulates in restricted areas, creating a pattern of inhomogeneous concentration. The experimental observation of a sustained standing non-equilibrium chemical pattern has been reported recently [26]. The possibility of such distinct qualitative behaviour makes autocatalytic systems attractive as a testing ground of the model developed here. It should be clear at the outset that the formation of structured states is predicted by the macroscopic diffusion-reaction equations. Linear stability analysis provides, in fact, a critical value, d_c , of the ratio of the inhibitor diffusion coefficient to that of the activator; when the ratio increases beyond d_c , a range of Fourier components of the concentration become unstable and appear as spatial oscillations with the corresponding wavelengths. The details of the transition, such as the value of d_c , may depend, however, on microscopic fluctuations and differences between the differential equation and CA approaches may appear [27]. Our aim here is to show that our model is universal enough to describe qualitative phenomena of the kind described above.

As a first example we consider the Brusselator [28], defined by the reaction scheme



Here the concentrations of A and B are kept constant and D and E are continuously removed. In this case, X is the activator and Y the inhibitor. The Brusselator, albeit

relatively simple, displays the striking qualitative behaviour (concentration oscillations in time and space, nonlinear travelling waves) exemplified by the Belousov-Zhabotinski reaction [29]. We consider a one-dimensional system of length L . Following Ref. [25], one can put the reaction-diffusion equations for the unconstrained concentrations in a dimensionless form,

$$\frac{\partial \tilde{C}_X}{\partial \tilde{t}} = \tilde{D}_X \frac{\partial^2 \tilde{C}_X}{\partial \tilde{x}^2} + \tilde{C}_A - (\tilde{C}_B + 1)\tilde{C}_X + \tilde{C}_X^2 \tilde{C}_Y \quad (3.5a)$$

$$\frac{\partial \tilde{C}_Y}{\partial \tilde{t}} = \tilde{D}_Y \frac{\partial^2 \tilde{C}_Y}{\partial \tilde{x}^2} + \tilde{C}_B \tilde{C}_X - \tilde{C}_X^2 \tilde{C}_Y \quad , \quad (3.5b)$$

by the transformation $\tilde{t} \equiv k_4 t$, $\tilde{x} \equiv x/L$, $\tilde{D}_{X,Y} \equiv D_{X,Y}/k_4 L^2$, $\tilde{C}_A \equiv (k_1 k_3^{1/2}/k_4^{3/2})C_A$, $\tilde{C}_B \equiv (k_2/k_4)C_B$ and $\tilde{C}_{X,Y} \equiv (k_3/k_4)^{1/2}C_{X,Y}$. Since C_B is held fixed and D plays no active rôle, the second reaction in the original scheme can be effectively replaced by $X \rightarrow Y$, with rate constant $k_2 C_B$.

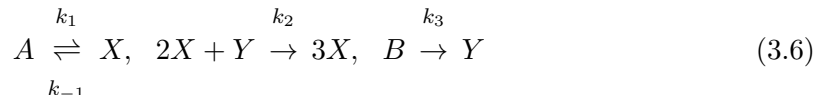
Fig. 8 shows the result of a simulation of Eqs. (3.5) on a one-dimensional lattice of length $1.01L$ (1010 sites, $\tilde{\lambda} \equiv \lambda/L = 10^{-3}$). We choose the physicochemical parameters to have the values quoted in Fig. 7.13 of Ref. [24]: $\tilde{C}_A = 2$, $\tilde{C}_B = 4.6$, $\tilde{D}_X = 1.6 \times 10^{-3}$ and $\tilde{D}_Y = 3.75 \tilde{D}_X$ ($d_c = 3.05$). The dimensionless concentrations $\tilde{C}_{X,Y}$ are computed by averaging the particle densities over cells of 10 sites and multiplying them by a scaling factor $\gamma \simeq 0.2$; to obtain $C_{X,Y}$, we multiply by an additional factor $(k_4/k_3)^{1/2}$. We constrain the boundary concentrations \tilde{C}_X and \tilde{C}_Y to remain fixed at the values of the (unstable) homogeneous steady state, i.e. \tilde{C}_A and \tilde{C}_B/\tilde{C}_A respectively; this is done as follows: before every iteration step, we replace all particles in the first and last cells by uniform random distributions of particles having the necessary density. Initially X - and Y -particles are distributed uniformly in the interior cell region of the lattice with densities of 9.2 and 10.7 particles/site respectively. The above value of γ is chosen to give initial concentrations of 1.8 and 2.1 respectively. In the simulation we face a problem of competing reactions (e.g. a single X -particle may either convert to a Y -particle or decay). Thus, in a naive implementation, in which all reactions are given a chance to take place one after the other, the order in which this is done would be significant. We solve the problem by dividing up reactions in groups of competing reactions and allowing randomly only one reaction from each group to take place during an iteration step (the probability of each

Figure 8: Simulation of one-dimensional Brusselator (solid curve) compared with solution of reaction-transport equations (dotted curve).

Figure 9: Spatial concentration pattern obtained from simulation of two-dimensional Schnackenberg model; regions of high (low) density are indicated in red (blue).

reaction has to be multiplied of course by the number of members in its group). For the parameter values chosen, the initial homogeneous state is unstable and the system evolves to a structured state. The spatial structure shown is obtained after 800 000 iterations with time step $\tilde{\tau} \equiv k_4\tau = 0.833 \times 10^{-4}$. Obviously the statistics is still poor for a quantitative comparison with the continuum result, which, incidentally, has converged to a stationary value by the time shown here.

The concentration pattern shown in Fig. 9 is produced with the reaction scheme



(Schnackenberg model [30]). The simulation is performed on a 696×721 lattice of size 1.10×1.14 (arbitrary units). Initially X - and Y -particles are distributed randomly, with uniform density 1.55 and 0.59 particles/site respectively. Other parameters are chosen as in Fig. 2a of Ref. [31]: $C_B = 1.41 k_1^{3/2} / k_3 k_2^{1/2}$, $C_A = 0.14 k_1^{3/2} / k_{-1} k_2^{1/2}$, $D_X = 10^{-4} k_1 L^2$ (L being the linear size of the system). Finally we take $D_Y = 30 D_X$ ($d_c \simeq 20$). The density of X -particles is shown here after 4800 iterations, with $\tau = 0.625 \times 10^{-6} k_1^{-1}$. Time limitations have prevented us from running the simulation up to a time when the pattern becomes stationary. CA simulation of spatial patterns with the Schnackenberg model has recently been reported by another group [27].¹¹

¹¹We have also performed simulations of the Selkov reaction scheme, which was introduced in the context of glycolytic oscillations and is obtained from (3.6) by making all reactions reversible [32]. We obtain concentration patterns, in agreement with Ref. [33], both above and below the critical diffusion-coefficient ratio. Below the critical ratio, the homogeneous state is apparently destabilised by density fluctuations which effectively widen the range of unstable wavenumbers.

4 Conclusion and Outlook

Reaction-transport processes were modelled in this work as a cellular automaton. Particles are transported by executing a random walk on the sites of a regular lattice and are chemically transformed according to a local probabilistic rule. The microscopic random motion of the particles is manifested, at the macroscopic level, as a combination of advection and diffusion. In particular, advection arises from a directional bias in the random walk, i.e. if particles have a relatively higher probability to move in the direction of the advection velocity. Chemical reactions are likewise modelled at the microscopic level: in the process of the random walk, we allow particles that meet at a lattice site the chance of ‘reacting’, i.e. disappearing and leaving in their wake a set of new particles, the products of the reaction. The model is *simple* and *general*. The evolution equations are transcribed into simple computer code. This simplicity does not preclude, but, on the contrary, facilitates the implementation of arbitrarily complex reactions and boundary conditions, in a physically transparent way. The results of the previous section demonstrate that the model presented here *can successfully describe a wide variety of reaction-transport systems*.

In the continuum limit, the evolution equations of the discrete model go over to the standard reaction-transport PDE’s, if certain conditions are fulfilled, namely if molecules of different species are uncorrelated (molecular chaos) and if particle density is smooth in space. These conditions are, however, not imposed in our model; thus our simulations account for microscopic effects (e.g. fluctuations) that are typically averaged out by the continuum approach. The results of the discrete model were compared carefully to the solution of the reaction-transport PDE’s in the case of a simple homogeneous system of particles. We encountered two sources of discrepancy: on the one hand correlations between the particles, that have no physical significance and are mere artifacts of the discretisation, and, on the other hand, statistical fluctuations that influence the long-time behaviour of reaction-diffusion systems. We emphasise the latter kind of discrepancy, which is of a fundamental nature and shows that microscopic fluctuations can influence qualitatively the evolution of macroscopic systems. The differences between the discrete simulation and the continuum approach in the time development of the reaction front

forming when the reacting species are initially separated is probably of similar origin. Macroscopic consequences of microscopic fluctuations were also seen in the case of autocatalytic reaction-diffusion systems, near the threshold for the onset of non-equilibrium phase transitions leading to formation of spatially structured states. We have thus shown in concrete cases that the discrete model *can be used to approximate systematically the respective PDE's, while, unlike the latter, it accounts for effects of explicitly microscopic origin.*

An important aspect of our approach is that the same macroscopic behaviour can be obtained with a variety of microscopic rules. This freedom is inherent in CA modelling, since the aim is to model only certain fundamental features of the microscopic world, but not the full detail of the dynamics. As examples, we gave two such rules: rule I, a simple rule leading to the standard rate law only in the limit of small densities, and rule II, a more complicated rule that, however, results in the standard rate law for any density. The computation time required by different rules in order to simulate the same macroscopic behaviour may vary. Our comparison of chemical rules I and II indicates that the latter affords better possibilities of optimisation, due to the wider range of possible particle densities.

Finding the optimal microscopic rule is one way of enhancing computational efficiency, which is an essential task in practical applications. As a consequence of the unlimited number of particles per site, our model does not vectorise well when implemented on computers with vector architecture. In the present general form of the model, the best scalar performance is attained on a VAX-9000 and amounts to $\sim 1\,000\,000$ site updates per second (u.p.s.) for pure transport of one species, $\sim 100\,000$ u.p.s. for $a + b \rightleftharpoons c$ and $\sim 20\,000$ u.p.s. for the Brusselator. This performance can be improved by varying the particle density, as we saw in Section 3. However, our model should be implemented on a massively parallel computer in order to achieve its full potential. The great advantage of our model is its ability to model a very wide range of reaction-transport problems. The performance figures quoted above are thus for a correspondingly general code. For specific applications, both the model and corresponding code can be appropriately tailored to optimise performance still further (see for example Ref. [13] where $20\,000\,000$ u.p.s. were

achieved on a CRAY-YMP for a specific reaction-diffusion process).

An important feature of our CA approach is its inherent stability. Indeed our algorithm is stable even for values of τ and λ for which the corresponding FDE's, represented by Eqs. (2.34) and (2.33), are numerically unstable when solved by direct iteration with particle densities being floating point variables. We note that adding chemical reactions to a problem of pure transport can turn a stable FDE algorithm into an unstable one - for the same time and space discretisation ¹². In such cases, where deterministic methods using floating point numbers fail, our stochastic approach, using integer variables, provides a stable method of solving Eqs. (2.34) and (2.33). The lack of general stability criteria for FDE in the presence of chemical reactions makes this guaranteed stability of our approach a valuable asset.

Realistic applications will constitute the principal direction of further work on our model. These applications will be chosen on grounds of practical usefulness and so as to utilise the advantages of our approach: the guaranteed numerical stability and the capacity to treat arbitrary boundary conditions and chemical systems which are not necessarily in chemical equilibrium. Thus applications will include both problems at field scale, where differential equations are used widely to describe average quantities, as well at the scale of the pores, which form networks with very complex boundary conditions. As examples we mention the chemistry of mineral surfaces (precipitation/dissolution) and the effects of porosity changes on mass transport [34].

In conclusion, we have shown that the cellular automaton model we are proposing is capable of simulating simple as well as complex reaction-transport processes. We understand well its relation to other numerical methods for solving the corresponding differential equations and will proceed to apply it to realistic problems. Where other methods work as well, the relevant question will be that of the relative computational efficiency. More challenging will be, however, to identify areas of application where differential equation approaches are confronted with either serious numerical or even conceptual problems.

¹²Stability is then achieved by refining further the time discretisation.

Acknowledgements

We would like to thank J. Hadermann for his interest in our work and C. L. Carnahan for a critical reading of the manuscript. Partial financial support by NAGRA is gratefully acknowledged. One of the authors (T.K.) has benefited a great deal from discussions with B. Chopard, M. Droz, L. Frachebourg, J.-P. Boon and D. Dab.

References

- [1] B. Blankleider, PSI Internal Report TM-41-90-13, Würenlingen and Villigen (1990).
- [2] T. Karapiperis and B. Blankleider, PSI Internal Report TM-41-91-42, Würenlingen and Villigen (1991).
- [3] S. Wolfram, *Rev. Mod. Phys.* **55**(1983)601.
- [4] J. Bear, *Hydraulics of Groundwater* (McGraw-Hill, New York, 1979).
- [5] G. T. Yeh and V. S. Tripathi, *Water Resour. Res.* **25** (1989)93;
D. C. Melchior and R. L. Bassett, eds., *Chemical Modelling of Aqueous Systems II* (American Chemical Society, Washington, DC, 1990).
- [6] T. Toffoli, in *Cellular Automata*, ed. D. Farmer *et al.*, *Physica D* **10**(1984)117.
- [7] B. M. Boghosian, *Comp. in Physics* **4**(1990)14.
- [8] D. Farmer, T. Toffoli and S. Wolfram, eds., *Cellular Automata*, Proc. of an Interdisciplinary Workshop, Los Alamos, March 1983, *Physica D* **10**(1984), Nos. 1 & 2;
S. Wolfram, ed., *Theory and Applications of Cellular Automata*, Adv. Series on Complex Systems, Vol. 1 (World Scientific, Singapore, 1986);
P. Manneville, N. Boccara, G. Y. Vichniac and R. Bidaux, eds., *Cellular Automata and Modeling of Complex Physical Systems*, Proc. of the Winter School, Les Houches, February 1989 (Springer, Berlin, 1989).
- [9] J. Hardy, O. de Pazzis and Y. Pomeau, *Phys. Rev. A* **13**(1976)1949.
- [10] G. Doolen, U. Frisch, B. Hasslacher, S. Orszag and S. Wolfram, eds., *Lattice Gas Methods for Partial Differential Equations*, Santa Fe Institute Studies in the Science

- of Complexity (Addison–Wesley, 1990);
- G. Doolen, ed. *Lattice Gas Methods for PDE's: Theory, Applications and Hardware*, Proc. of the NATO Advanced Research Workshop, Los Alamos, September 1989, *Physica D* **47**(1991), Nos. 1 & 2.
- [11] U. Frisch, B. Hasslacher and Y. Pomeau, *Phys. Rev. Lett.* **56**(1986)1505.
- [12] A. Lawniczak, D. Dab, R. Kapral and J.-P. Boon, *Physica D* **47**(1991)132.
- [13] B. Chopard and M. Droz, *Europhys. Lett.* **15**(1991)459.
- [14] T. Toffoli and N. Margolus, *Cellular Automata Machines: A New Environment for Modeling* (MIT Press, Cambridge, 1987).
- [15] B. M. Boghosian and C. D. Levermore, *Complex Systems* **1**(1987)17.
- [16] B. J. Noye, in *Numerical Simulation of Fluid Motion*, ed. B. J. Noye (North–Holland, South Australia, 1978), pp. 1–112.
- [17] C. D. Levermore and B. M. Boghosian, in *Cellular Automata and Modeling of Complex Physical Systems*, ed. P. Manneville *et al.* (Springer, Berlin, 1989), pp. 118–129.
- [18] D. Dab and J.-P. Boon, in *Cellular Automata and Modeling of Complex Physical Systems*, ed. P. Manneville *et al.* (Springer, Berlin, 1989), pp. 257–273.
- [19] W. Feller, *An Introduction to Probability Theory and its Applications* (Wiley, New York, 1970).
- [20] D. Toussaint and F. Wilczek, *J. Chem. Phys.* **78**(1983)2642.
- [21] B. Chopard, M. Droz, T. Karapiperis and Z. Rácz, *Phys. Rev.* **E 47**(1993)40.
- [22] L. Gálfi and Z. Rácz, *Phys. Rev.* **A 38**(1988)3151.
- [23] S. Cornell, M. Droz and B. Chopard, *Phys. Rev.* **A 44**(1991)4826.
- [24] G. Nicolis and I. Prigogine, *Self-Organization in Nonequilibrium Systems* (Wiley, N. York, 1977).
- [25] J. D. Murray, *Mathematical Biology* (Springer, N. York, 1989).

- [26] V. Castets, E. Dulos, J. Boissonade and P. de Kepper, Phys. Rev. Lett. **64**(1990)2953.
- [27] M. Droz and L. Frachebourg, Helv. Phys. Acta **66**(1993)97.
- [28] I. Prigogine and R. Lefever, J. Chem. Phys. **48**(1968)1695.
- [29] B. P. Belousov, Sborn. Referat. Radiat. Med. 1958 (Moscow, 1959), p. 145;
A. M. Zhabotinski, Dokl. Akad. Nauk SSSR **157**(1964)392.
- [30] J. Schnackenberg, J. Theor. Biol. **81**(1979)389.
- [31] V. Dufiet and J. Boissonade, J. Chem. Phys. **96**(1992)664.
- [32] E. E. Selkov, Eur. J. Biochem. **4**(1968)79.
- [33] R. Kapral, A. Lawniczak and P. Masiar, Phys. Rev. Lett. **66**(1991)2539.
- [34] D. H. Rothman, Geophys. **53**(1988)509;
S. Chen, K. Diemer, G. D. Doolen, K. Eggert, C. Fu, S. Gutman and B. J. Travis,
Physica **D 47**(1991)72;
J. T. Wells, D. R. Janecky and B. J. Travis, *ibid.* **D 47**(1991)115.